

R-06-103

Physical and chemical stability of the bentonite buffer

Jinsong Liu, Ivars Neretnieks
Chemical Engineering and Technology
Royal Institute of Technology

December 2006

Svensk Kärnbränslehantering AB

Swedish Nuclear Fuel
and Waste Management Co
Box 5864

SE-102 40 Stockholm Sweden

Tel 08-459 84 00
+46 8 459 84 00

Fax 08-661 57 19
+46 8 661 57 19



ISSN 1402-3091

SKB Rapport R-06-103

Physical and chemical stability of the bentonite buffer

Jinsong Liu, Ivars Neretnieks
Chemical Engineering and Technology
Royal Institute of Technology

December 2006

This report concerns a study which was conducted for SKB. The conclusions and viewpoints presented in the report are those of the authors and do not necessarily coincide with those of the client.

A pdf version of this document can be downloaded from www.skb.se

Abstract

Bentonite clay intended for use as a buffer around the waste canisters will form a stable gel under the expected groundwater compositions at potential repository sites. A literature survey has been made of the forces involved that attract and those that repel the clay particles under different conditions. Especially the repulsive forces and how these are influenced by the water chemistry have been studied, because in low ionic strength waters these forces can become so strong that the gel becomes unstable. Results from measurements described in the literature are also presented.

The bentonite backfill surrounding the waste canister may be eroded by swiftly flowing water in the fractures that intersect the deposition hole. The clay gel acts as a Bingham fluid and there is a minimum shear stress that water must exert on the gel to mobilise the particles. The shear stress at the gel/water interface has been estimated for a wide range of hydraulic conditions that could be expected even under very high gradients that could be generated by a receding ice front during an ice age. The shear stress has been compared to the Bingham yield stress. The latter is influenced both by the pore water chemistry as well as by the density of the clay gel.

The stability of the clay is strongly influenced by the calcium and other divalent cation concentrations in the pore water. If the clay is exposed to water with a calcium concentration that is lower than the critical coagulation concentration, the CCC, the clay gel can form a sol and the clay particles can be carried away by the passing water.

Using boundary layer theory for diffusing species we have calculated the rate of transport of calcium from the clay to a groundwater that flows and contacts the clay in the fractures that intersect the deposition hole. Based on this a simple illustrative entity called the equivalent flowrate is introduced and used to derive a simple expression that relates the loss of clay to the hydraulic properties, the CCC, the content of soluble calcium minerals and to the composition of the approaching groundwater.

Summary

Previous work

A literature study was made on previous work on clay erosion and on the fundamental processes that govern the stability of clay gels. Mechanical erosion has been studied earlier and models devised to estimate the tendency to erode. We have used a different approach that we deem is fundamentally more correct. Chemical erosion processes have not been found to be studied previously and we have approached the problem by applying simple but fundamental mass balances and transport processes to the problem.

The physical and chemical processes that govern the repulsive and cohesive forces in clay are well understood in principle but cannot yet be applied quantitatively to predict the gel/sol behaviour of the bentonite clay. It was necessary to rely directly on laboratory measurements for information on swelling and gel/sol properties.

Mechanical erosion

The backfill bentonite clay acts as a Bingham fluid over a wide range of clay density. To mobilise the clay a shear stress larger than the Bingham yield stress must be applied to the gel. The Bingham yield stress has been measured to be larger than 1 Pa (N m^{-2}) although it cannot be ruled out that lower values can be found under different experimental conditions than those reported.

Shear stresses exerted by the water flowing in the fractures that intersect the deposition holes with the clay backfill have been estimated for a wide range of fracture transmissivities, apertures and hydraulic gradients that could exist under repository conditions. This includes the extremely high gradients that could exist during some periods during an ice age.

For fracture transmissivities ranging from 10^{-9} to $10^{-6} \text{ m}^2 \text{ s}^{-1}$, fracture apertures from 0.1 to 2 mm and the hydraulic gradients from 0.01 to $1 \text{ mH}_2\text{O m}^{-1}$, the largest local shear stress found in this range was about 0.1 Pa.

To investigate a “what if” situation where the shear stress exceeds the yield stress simple models were devised. They were used to assess the rate of erosion by the groundwater. In one model it is assumed that the width and depth of the shear boundary layer is filled with the solubilised gel and flowing water simply shears off that portion of the gel. Under extreme conditions on the order of a tenth of a kilogram of clay could be eroded per year. In the other model the clay gel front is treated as a solute (when the shear stress exceeds the Bingham yield stress) with a clay particle diffusivity in the water. Boundary layer theory is used to determine how much clay “solute” could diffuse into the water that passes the deposition hole. The results are similar to those of the previous model.

We conclude that it is highly unlikely that mechanical erosion should take place even under rather extreme conditions in a repository that has been saturated with water.

Chemical erosion

The stability of the gel decreases with decreasing concentration of especially divalent cations and there is a critical coagulation concentration, CCC, under which the gel becomes a dispersion, called a sol. The main divalent cation of interest in this context is calcium that is present in the clay pore water but also as soluble mineral gypsum or anhydrite. The solubilities of both gypsum and anhydrite are higher than the CCC and thus as long as there is gypsum or anhydrite in the clay, loss of calcium to a fresh groundwater that comes into contact with the clay can be replenished by dissolution of the gypsum or anhydrite. However, with time the mineral is exhausted in the clay nearest to the flowing water and the gel can form a sol, which is carried

away by the water. This exposes new gel to the flowing water and a steady state loss of clay can be attained. Other calcium minerals such as calcite have a much lower solubility than the CCC and will contribute less to the replenishing of calcium in the pore water.

We have approached the problem by modelling the rate of calcium transport from the interface between the clay gel and the water flowing in a fracture that intersects the deposition hole. Transport into the passing water is modelled using the diffusion equation for transport in the water flowing in the fracture. For the range of hydraulic and other variables, we have used a very simple analytical solution for the mass transfer. It is summarised and illustrated by the entity “equivalent flowrate” Q_{eq} . This entity describes the flowrate of water that would carry a concentration of solute equal to that at the gel/water interface. The Q_{eq} is determined by a very simple formula that summarises a number of complex processes, including varying diffusion into water passing a curved boundary.

The Q_{eq} depends in a simple way only on the transmissivity and aperture of the fracture, the hydraulic gradient and the size of the deposition hole.

For very fresh water approaching the clay the rate of loss of calcium from the clay gel is shown to be proportional the CCC and Q_{eq} . The rate of loss of clay is proportional to the loss of calcium and inversely proportional to the content of soluble calcium minerals (mainly gypsum) in the clay.

Sample calculations are given to illustrate how different entities influence the loss of clay. The range of parameter values are the same as for the physical erosion, namely: the fracture transmissivities from 10^{-9} to 10^{-6} $\text{m}^2 \text{s}^{-1}$, the fracture apertures between 0.1 and 2 mm and the hydraulic gradients from 0.01 to 1 $\text{mH}_2\text{O m}^{-1}$. In the sample calculations the approaching water is taken to have no calcium at all. The gypsum content is taken to be 0.7% by weight and the CCC to be 1 mmol L^{-1} (mM).

The rate of loss of clay varies from a few grams per year to some kg per year under the most extreme conditions, i.e. $T = 10^{-6}$ $\text{m}^2 \text{s}^{-1}$, fracture aperture 2 mm, and hydraulic gradient of 1 $\text{mH}_2\text{O m}^{-1}$.

Finally some very simple equations are given that can be used to calculate the physical as well as the chemical erosion. The equations are summarised in Chapter 5 of this report.

Contents

1	Introduction	9
2	Literature review	11
2.1	Bentonite expansion with water uptake and its intrusion into the intersecting fracture	11
2.2	Forces of particle interaction and the physical stability of the bentonite buffer	12
2.3	Modification of surface charges and chemical stability of the bentonite buffer	14
3	Modelling of physical stability of bentonite	17
4	Modelling of chemical stability of the bentonite	23
4.1	Conceptual model	24
4.2	The upper-bound limit calculation of the initial release rate of calcium	26
4.3	Modelling bentonite loss after the initial period	29
5	Summary of the models	35
5.1	Physical erosion	35
5.2	Chemical erosion	35
6	Discussion	37
7	Conclusions	39
	References	41

1 Introduction

In the KBS-3 concept of a spent nuclear fuel repository the long-term stability of the bentonite buffer is of vital importance for the retention of the radionuclides in the repository. The compacted bentonite buffer is the engineered barrier in the repository and is one of the important components in the multi-barrier system of the repository.

Compacted bentonite is composed mainly of sodium montmorillonite. Montmorillonite is a clay mineral of the dioctahedral smectite 2:1 group, consisting of sheets with a layer of octahedral aluminium oxide between two layers of tetrahedral silicon oxides. With uptake of water the bentonite buffer may expand under the swelling pressure of the clay, containing Na- and Ca-montmorillonite. As the buffer material is confined by the surrounding rocks in a deposition hole in a repository, the volumetric expansion will be limited. The volume increase will be essentially due to the intrusion of the clay into the fracture(s) in the surrounding rock that may intersect the canister. A balance between the swelling pressure and the friction of the intruding clay and the fracture planes will determine the depth of the intrusion.

During water uptake, looser clay gels may form where the density of the bentonite decreases. The looser gels will mainly form at the front of the clay intrusion in the fracture as the density is expected to be lowest there. When the coagulation force of the gel front becomes less than the drag force exerted by the flowing groundwater in the fracture, the gel front will be eroded and be carried away by the flowing groundwater. This is the physical instability of the bentonite buffer considered in the present report.

Moreover, the stability of the gel front, in some cases the entire intrusion or even the inside bentonite proper, depends strongly on the chemical composition of the pore water of the bentonite. The pore water composition will gradually change with time if the groundwater in contact with the buffer is not in equilibrium with the pore water. During the downward penetration of glacial waters at a time of glaciation retreat, the clay gels may become chemically unstable while in contact with the water of very low ionic strength. The chemical stability of the bentonite depends especially on the divalent cation concentrations in the pore water of the bentonite. When the bentonite initially contains minerals of relatively high solubilities of divalent cationic species, such as gypsum or anhydrite, the calcium cation concentration in the pore water will be buffered by the dissolution of these minerals and be above the critical coagulation concentration (CCC) of the montmorillonite. When these calcium containing minerals are depleted by diffusion to the passing water, the calcium concentration in the pore water of bentonite may drop below the CCC and the gels may disperse into the water as colloidal particles and be also carried away by the flowing groundwater. This is the chemical instability of the bentonite buffer considered in this report.

Loss of the bentonite buffer may have severe consequences for the performance of the entire repository, e.g. it may allow more corrosive water (containing S^{2-}) to contact the copper canister and speed up the attack on the canister. Also with the loss of bentonite after the breach of the metal canister, radionuclides of fission products and some actinides may be released faster from the breached canister. Furthermore the nuclides may sorb on the clay colloid surface and their transport in the fracture water may be considerably enhanced (Buddemeier 1988, Mōri et al. 2003). A significant loss of the bentonite buffer may also reduce the radionuclide retention capacity of the entire multi-barrier system of the repository concept, as radionuclide transport and release through an intact bentonite buffer are molecular diffusion processes and extremely slow.

In this report, we will first present a literature review of some of the theoretical as well as experimental works on physical and chemical stabilities of the bentonite clay. We then make some bounding calculations concerning the physical stability of the bentonite buffer under

repository conditions, by considering the force balance of the yield stress of the bentonite and the drag force of the flowing groundwater in the fracture. We then proceed to calculate the chemical stability of the bentonite buffer, taking into account of different chemical compositions of the bentonite buffer.

The aims of the report are (1) to study the physical stability of the bentonite buffer, i.e. the erosive resistance of the gel front of the bentonite intruding into the fracture, and (2) to study the chemical stability of the bentonite buffer when the groundwater in the fracture becomes extremely low in ionic strength.

2 Literature review

2.1 Bentonite expansion with water uptake and its intrusion into the intersecting fracture

The bentonite buffer material consists mainly of Na- and Ca-montmorillonite, with small amounts of other minerals such as quartz, feldspars, zeolites, calcite/siderite, gypsum/anhydrite, and pyrite. Two different types of bentonite are considered as reference buffer material in a recent interim report of SKB, which aims at supporting SKB's license application to build an encapsulation plant for spent nuclear fuel: the natural mainly Na-bentonite of Wyoming type (MX-80) supplied by the American Colloid Company, and a natural mainly Ca-bentonite (Deponit CA-N) from Milos, Greece, supplied by Silver and Baryte /SKB 2004/. The detailed compositions, especially the amounts of the calcium-containing minerals of the two types of bentonite vary and we will address this issue in a later section of this report. For the buffer, freshly compacted bentonite has a bulk density of about 1,600 to 1,800 kg m⁻³ and a water content of about 10% by weight. The compact bentonite retains the fine structure of the bentonite powder that forms it. Commercial bentonite powders of the MX-80 type are very dense aggregates of silt/sand size (with a mean value of about 0.16 µm). The aggregates consist of parallel-oriented *laminae* (synonymously also called *lamellae*, *platelets*, sometimes even informally "*plates*", in the literature) of montmorillonite crystals. In the compact bentonite as well as in the bentonite powder, the intra-aggregate spacing is very small and the inter-aggregate spacing (the pores) is fairly large /Pusch 1983, Pusch 1999, Pusch and Adey 1999/.

In the course of water saturation the aggregates expand and, after a sufficiently long time, most of the larger voids (the inter-aggregate pores) will be partly or entirely filled by the clay gel emerging from the expanding aggregates. The aggregate expansion results in a swelling pressure. When the bentonite is confined in space, as is the situation in a spent fuel repository, the degree of expansion is small and the physical properties of the bentonite are relatively isotropic and homogeneous. At not too high water saturation the initial condition of parallel orientation of the thin laminae in the individual aggregates will be preserved while the spacing between the laminae will be increased /Pusch 1983/.

The increase of the spacing between the laminae in the bentonite aggregates (intra-aggregate spacing) is a result of crystal lattice expansion during the uptake of water. The water molecules will be coupled to the basal plane of a lamina and the near-surface water film "crystallise" to give looser structural arrangement of the water molecules. It has been shown /Forslind and Jacobsson 1973/ that the hydration stages seem to be relatively unaffected by the pore water chemistry for water contents lower than about 35%, which corresponds to 3 ordered water molecule layers. The swelling pressure is also relatively little affected by the water compositions under the above level of water uptake, which implies that the pressure is mainly due to the structural changes of the intra-lamellar water. The stability of the structural lattice water drops rapidly when the distance between basal planes of the laminae of the bentonite increases, and the influence of the structural water on swelling pressure then becomes negligibly small.

The relatively free expansion of the spacing between the laminae of Na-montmorillonite may result in significant deviation from the original parallel arrangement of the laminae and therefore the volume may increase many times. During expansion Ca-montmorillonite preserves its original parallel arrangement of the laminae and therefore shows more limited swelling. Similar results have been observed for potassium as a counterion. As K⁺ is less hydrated compared with Na⁺, it readily migrates and binds to the clay surface to shield the negative charges on the surface, and thus effectively reduces the repulsive forces and decreases the tendency of K⁺-saturated clay to expand /Boek et al. 1995/.

With certain groundwater compositions (low ionic strengths), the aggregates in the bentonite powders or gel can be completely dispersed to form sols of individual flakes of the constituent laminae with a thickness of about 1 nm. This issue will be considered later.

/Boek et al. 1995/ have suggested that two types of swelling should be distinguished in relation to clay hydration: (1) *intracrystalline* swelling, involving the adsorption of limited amounts of water in the interlayer (intra-lamellar) spacing, and (2) *osmotic* swelling, related to unlimited adsorption of water due to the difference between ion concentrations close to the clay surface and in the pore water. Osmotic swelling occurs probably only when the water uptake in the bentonite becomes large.

When a deposition hole in a repository is intersected by a fracture, the swelling bentonite will intrude into the fracture. In a model proposed by /Pusch 1983/ the penetration was considered to be the net effect of two different mechanisms: (1) Swelling due to water uptake, (2) Retardation due to wall friction effects. The friction effects were modelled by adapting a stepwise methodology to account for the variation of the viscosity of bentonite with density. The intrusion rate is a function of the density of the bentonite and the aperture size of the fracture /Pusch 1983/. The modelling results of the intrusion depth into the fracture indicate that, for fracture apertures between 0.1 and 0.5 mm, the depth could be 0.3 cm to 7.5 cm after 10^6 years. Further consideration of the effect of the temperature on the viscosity of the bentonite buffer results in much larger intrusion depths, at least 10 cm of bentonite with an average density of $1,500 \text{ kg m}^{-3}$ for all apertures after a few hundred years. Experimental results also confirmed this conclusion /Pusch 1983/.

2.2 Forces of particle interaction and the physical stability of the bentonite buffer

During the intrusion of the bentonite buffer into the intersecting fracture, the density of the clay in the fracture will decrease as a result of expansion. A zone of clay gel will be formed at the front of the intruding bentonite as the density there becomes the lowest. The gel front was observed in experiments to be thin and soft, while the rest of the intruding clay is relatively stiff /Pusch, 1983/. In this report the physical stability of the bentonite is meant to be the stability of the gel front of the intruding clay under the drag force exerted by the flowing groundwater in the fracture.

The physical stability of the bentonite buffer is usually characterised by the balance of the interactions of clay particles (the laminae or aggregates) and the drag force of the groundwater flow. It will be seen later that the chemical stability of the bentonite clay is also determined by the interactions of clay particles. In consideration of the chemical stability, however, we focus on the changes (often weakening) of the clay particle interactions by the change of pore water chemical compositions and the dispersion of the gel front.

The gel front of the intruding bentonite in the fracture can possibly be eroded by the flowing groundwater in the fracture if the drag force of the flow water is larger than the force of clay particle interactions. As long as the gel has not been dispersed as sols by changing chemical compositions of the groundwater, the erosion rate will be determined by the gel's shear strength as well as the flowrate of the groundwater, which exerts a shear force on the gel surface.

When the laminae in the clay aggregates are no longer parallel with large amount of water uptake, the inter-laminar force fields are changed. The bonds between the laminae become weak as a result of the expansion. Three modes of association of the bentonite laminae are now possible: face-to-face (FF), edge-to-edge (EE) and edge-to-face (EF) /M'bodj et al. 2004/. The face here indicates the facial plane of the 2:1 phyllosilicate sheet of a clay lamina. The edges are boundaries of the sheet other than the facial plane. These three types of interactions cause the clay laminae to flocculate and form gels when the chemical conditions favour this. Theoretical description of the particle interaction by the Derjaguin-Landau-Verwey-Overbeek

(DLVO) /Verwey and Overbeek 1948/ theory (interaction between electrical double layer repulsion and the London-type van der Waals force attraction) has been found to be in reasonable agreement with many experimental observations. The DLVO model probably can treat the FF interaction adequately. Yet it fails to give a complete picture, especially in accounting for the EE or EF associations of the laminae. It has not been found possible to use these models to quantitatively describe the balance between the repulsive and attractive forces on the bentonite buffer. Empirical relations based on direct measurements have to be used. However, the theoretical models give valuable insights into the qualitative behaviour of the clay, some of the theoretical considerations are summarised below.

In the clay lamina, there exist permanent charges of the silicate layers resulting from isomorphous ionic substitutions in the crystal lattice (Mg^{2+} and Al^{3+} for Si^{4+}). Such charges are hence essentially independent of the ionic composition of the medium in which the bentonite is dispersed. In contrast, the edges of the lamina originated by fracturing (breaking) of the crystal structure have a composition close to that of Al or Si oxides, and form surface hydroxyl functional groups (SOH) in water. Charges on the edge are therefore strongly pH dependent /Ramos-Tejada et al. 2001/. At the broken edge of the octahedral sheets positive charges may arise in acidic and neutral solutions. At the broken edge of the tetrahedral sheets positive charges may exist when small amounts of aluminium are present in the solution.

It has been postulated /van Olphen 1951, 1963, Lambe 1958/ that flocculation of clay particles could be a result of the interactions between positive charges present on the edge of clay laminae and negative charges on the face of the clay plates. /Missana and Adell 2000/ have shown that the small fraction of the pH-dependent charges on the edge greatly influence the stability behaviour of the clay colloids and that the DLVO theory is not particularly suitable to predict the stability, mainly because it is not able to account for this charge contribution. A significantly larger value of the Hamaker constant in the attractive potential of the van der Waals interaction has to be used to account for the experimental data. This value is unreasonably larger than that obtained from experimentally determined critical coagulation concentration (CCC) of Na-bentonite. /Missana and Adell 2000/ attributed the large discrepancy to other interactions, especially the edge-to-face (EF) interaction that are not accounted for by the DLVO theory. The EF aggregation is mainly an electrostatic interaction between the positively charged edge and the negatively charged face.

Other types of bonding mechanisms have also been assumed in the literature /Rosenqvist 1955/ for the particle interactions: (1) attraction caused by the asymmetrical distribution of the adsorbed cations to form electrostatic bonding, (2) van der Waals forces between polarised adsorbed cations, (3) attractive forces between cations adsorbed on one particle and the lattice field of an adjacent particle, (4) attraction by the action of the adsorbed polar molecules or hydrogen bonds.

As it is usually difficult to quantify the interactions of the clay aggregates, experiments have been made by many authors to directly determine the rheological properties of the buffer. A large number of publications concerning the rheological properties of the bentonite are available in the literature as bentonite has been intensively used in drilling fluids in the petroleum industry /e.g. Chilingarian and Vorabutr 1983, Darley and Gray 1991/.

As in other disperse systems, the rheological properties of bentonite are strongly correlated with the degree of flocculation between the particles and with the structure of the flocculi. The pioneering works of /Norrish 1954, 1972/ and /van Olphen 1956/ suggested that the mechanical strength of montmorillonite gels must be related to the formation of particle networks in which individual clay particles are in contact with others, forming ribbon-like or scaffolding structures. /Ramos-Tejada et al. 2001/ have recently studied the rheological behaviour of Na-montmorillonite suspensions. The behaviour is mainly due to the complex structure of the electric double layer surrounding the particles when they are in contact with aqueous ionic solution.

The rheological properties of the saturated clay have been studied by treating the clay as compressible fluid, under both Newtonian and non-Newtonian (often of Bingham type) assumptions

/Grindrod et al. 1999/. The yield stress of a sodium kaolinite with a clay concentration of 9.1% has been measured by /Nickel 1997/. The clay was dispersed in various concentrations of NaCl, ranging from 10^{-5} – 10^{-3} M for dispersed clay, $3 \cdot 10^{-3}$ – $3 \cdot 10^{-1}$ M for flocculated clay and 1–3 M for highly flocculated clay.

The yield stress of Wyoming bentonite (MX-80) has been measured by /Pusch 1983/ for different clay concentrations in different waters (distilled water, Allard water /Allard et al. 1983/, and NaCl and CaCl₂ solutions).

The yield stress, σ , and the elastic modulus, G , of a natural sodium bentonite from Almería, Spain, have been found to have a power-law relation with the concentration of the clay particles (% wt/vol) /Ramos-Tejada et al. 2001/. The power is between 2 and 5 for strongly flocculated suspensions and between 5 and 8 for stable or weakly flocculated ones.

The yield stress and the elastic modulus of a smectite-illite clay have been experimentally studied by /M'bodj et al. 2004/ to clarify the effects of the clay fraction, the salt concentration and the addition of a semigrad polymer, on the values of σ and G . They found that both the yield stress and the elastic modulus have a power-law relation with the clay volume fraction. Moreover, progressive addition of NaCl to the clay dispersions decreases the thickness of the diffuse double layer, which makes the system rigid, increasing the yield stress and the elastic modulus.

More detailed information including the values of the yield stress measured will be presented later in this report in Chapter 3: “Modelling of physical stability of the bentonite buffer”.

/Pusch 1983/ addressed the physical stability of bentonite by using a model of force balance on individual clay particles. First, the yield stress was used to derive a rough estimation of the particle bond strength. This was done by assuming a homogeneous clay gel, and by dividing the yield stress by the total number of particle contact per unit area to obtain an average strength of each particle interaction. The values were on the order of 10^{-13} N per interaction. The drag force exerted by the flowing groundwater was represented by the force born by each particle using Stoke's equation ($F = 3d\pi\eta \cdot v$) in which d is the diameter of the clay particle (m), η is the viscosity of the flowing groundwater (Pa s), and v is the groundwater velocity (m s^{-1}). The results showed that for typical groundwater velocities in a fracture ($< 10^{-5}$ m s^{-1}) and for the majority of the clay particles (with a size less than 0.5 μm) the drag force is much less than the interaction force of the particles and concluded that the clay is physically stable. Similar results have been found in a later study of the same author /Pusch 1999/.

2.3 Modification of surface charges and chemical stability of the bentonite buffer

The chemical stability of the bentonite buffer is closely related to its physical stability. Both physical and chemical stabilities are determined by the strengths of interactions between the clay particles. While the physical stability emphasises the influences of the external forces on the interactions, the chemical stability focuses on the influences of the chemical properties of the medium (in our case the chemical compositions of the groundwater) on the interactions, especially the modification of the surface charges (and hence the interfacial interactions) by the changing water compositions (e.g. its ionic strength and acidity/alkalinity).

It has been observed experimentally that there is an abrupt change from stability to instability of the bentonite gel coagulates or flocculi on changing the salt concentration of the medium (the water) /van Olphen 1977/. The electrolyte concentration at the changing point is termed critical coagulation concentration (CCC). In the DLVO theoretical framework, i.e. by assuming that the stability is the result of the interaction between the diffuse electrical double layer repulsion and the van der Waals attraction, the turning point of stability is the point at which the repulsive force balances exactly the attractive force and thus the mechanical potential (the force is defined

as the negative gradient of the mechanical potential) has a maximum. At this point the separation in distance will be equal to the Debye length ($1/\kappa$) between spherical particles and twice as large between parallel plates /Evans and Wennerström 1999/. As the Debye length is inversely proportional to the square root of the ionic strength, the chemical stability of clay coagulates or flocculi will therefore decrease with decreasing ionic strength. It should be noted that in this report we focus on the stability of the gels (coagulates or flocculi) that is actually the *instability* of the clay colloids that is usually the focus in the colloid chemical literature.

Within the DLVO theoretical framework, the CCC can be related to the surface electrical potential, to the dielectric constant of the medium, to the valence of the electrolyte of the medium, as well as to the Hamaker constant of the van der Waals interaction /Evans and Wennerström 1999/:

$$CCC \cong 4 \cdot 10^2 \frac{(\epsilon_0 \epsilon_r)^3 k_B T \phi_0^4}{(zeH_{121})^2} \quad (2-1)$$

where ϵ_0 is the electric permittivity in vacuum ($8.854 \cdot 10^{-12}$ F m⁻¹), ϵ_r is the relative electric permittivity or dielectric constant of water (78.5 at 25°C), k_B is the Boltzman constant ($1.38 \cdot 10^{-23}$ J K⁻¹), z is the valence of the electrolyte ions, e is the electric charge of an electron ($1.602 \cdot 10^{-19}$ C), T is the absolute temperature (K), ϕ_0 is the surface potential of the clay particle (V), and H_{121} is the Hamaker constant (J).

The CCC can usually be experimentally determined by adding salt solution into the clay dispersion in the turbidity measurement. When the dispersion concentration is high in the original colloid solution, the rheological method for measuring CCC is based on the fact that at the CCC the viscosity of the dispersion increases sharply.

The CCC of 5–10 mM sodium counterions for Na-montmorillonite dispersions is extremely low, compared with the usual values between 25 and 500 mM for other clay minerals /Verwey and Overbeek 1948, Lagaly et al. 1997/. For divalent counterions like Ca²⁺, the CCC for Na-montmorillonite is about 1 mM /Pusch 1983, SKB 2004a/. The observation of the relatively low CCC values for Na-montmorillonite was explained by the interaction of positive edge charges with negative face charges producing T-type contacts and aggregation in card-house type arrangement /van Olphen 1977/. /Lagaly and Ziesmer 2003/ observed that, at pH near or higher than the point of zero charge (pzc) of the edges, i.e. positive charges are no longer present at the edges (the edges become negatively charged), coagulation still occurs between edges (–) and faces (–). In addition to the pH influences, the negative double layer extending from the basal plane (the face) surfaces may “spill over” into the edge region when the Debye length of the double layer becomes significantly larger than edge thickness and thus diminish the effect of the positive charges at the edges. As the negative edge charge density is very small, coagulation requires low sodium salt concentrations (low CCC). Even by assuming that the edge charge density is the same as that of the face charge, calculations by the DLVO theory still showed that the repulsion is distinctly smaller between EF interaction than between FF interaction /Pierre 1992/. This study by /Pierre 1992/ implies that, even at higher pH values, the EF interaction may still be a dominating factor for the coagulation of the Na-montmorillonite colloids at low ionic strengths (or salt concentrations).

Most studies on colloid stability were made by following the relationship between the changes only of the surface electric charges of the particles represented most often by their zeta potentials or electrophoretic mobility and that of the stability of the dispersed system. It has been, however, of considerable interest in the literature to broaden the correlation studies by including also the correlation between variations of the electric moments of the surface charges and the colloid stability. Thus besides total surface charges their distribution and dynamics should also be considered. This particular issue has been intensively reviewed by /Stoylov 1994/.

A natural bentonite often contains calcium minerals like gypsum or anhydrite (often also calcite) which, when dissolved, can function as a source of calcium cations in the pore water of the bentonite. When such a bentonite is used as a buffer material in a repository, the Na-montmorillonite will not disperse to colloids when initially in contact with groundwaters of low ionic

strengths. The solubilities of these calcium minerals are usually higher than the divalent cation CCC of the Na-montmorillonite /Wanner et al. 1992, Wieland et al. 1994, Bruno et al. 1999/.

/Bruno et al. 1999/ have studied quantitatively the chemical evolution of the buffer as a result of the interactions of the intruding groundwater with the MX-80 bentonite main components and accessory minerals. The following processes have been considered in their study: (1) dissolution of anhydrite and calcite, (2) ion-exchange reactions at the facial sites, (3) surface protonation and complexation reactions at the edge silanol and aluminol sites, (4) montmorillonite weathering reactions, (5) redox buffering reaction of the pyrite or siderite. The first three processes were modelled with chemical equilibrium approach while the last two were modelled by chemical kinetics.

Dissolution of the calcium-containing minerals during initial equilibrium of bentonite with groundwaters will result in cation-exchange reactions for the calcium cations to replace the original sodium cations in the facial diffuse double layers, even for waters that are low in calcium concentration /Bruno et al. 1999/. For example, the initial Ca^{2+} concentrations in the Swedish Äspö, Finnsjön and Gideå groundwaters are $4.73 \cdot 10^{-2}$, $3.55 \cdot 10^{-3}$ and $5.25 \cdot 10^{-4}$ M respectively. After equilibrium with the MX-80 bentonite of a total content of calcium minerals of 1.4% (wt), the final concentration of Ca^{2+} in the pore waters become $3.71 \cdot 10^{-3}$, $2.04 \cdot 10^{-3}$ and $1.96 \cdot 10^{-3}$ M, respectively /Bruno et al. 1999/. When the Ca^{2+} concentration in the initial water is high, less calcium minerals will dissolve than required for the cation-exchange of Na^+ and the Ca^{2+} concentration in the water decreases after equilibrium with the bentonite clay. When the initial water has lower concentration of Ca^{2+} , the opposite will be true. In any case, it seems that the final Ca^{2+} concentration in the water will be larger than the CCC concentration of the Na-montmorillonite which is $1 \cdot 10^{-3}$ M when the bentonite is initially equilibrated with the above three types of groundwaters.

The chemical evolution of the bentonite in contact with different groundwaters has also been modelled by /Bruno et al. 1999/. Their results indicated that the concentration of the Ca^{2+} in the groundwaters is of great significance. When the Ca^{2+} is high as is the case for the Äspö groundwater, the Na-bentonite could be completely converted to Ca-bentonite through cation-exchange reactions within 0.5 million years. While for the Gideå groundwater with a low concentration of Ca^{2+} , the depletion of gypsum or anhydrite, and eventually even calcite in the bentonite could not be compensated by the slow Na-Ca exchange reactions and the pH values will increase to 10.5 after 1 to 1.5 million years.

One important finding of /Bruno et al. 1999/ is that the calcite present in the bentonite is only dissolved marginally when the bentonite is equilibrated with Äspö, Finnsjön and Gideå groundwaters. The presence of soluble calcium containing minerals has a strong impact on the chemical erosion of bentonite as will be demonstrated later.

3 Modelling of physical stability of bentonite

The term of physical stability has a very narrow connotation in this report as has been discussed earlier. The front part of the bentonite intruding into the intersecting fracture is usually in a gel form and is very soft compared to the other part of the bentonite buffer. When subject to the shear force exerted by the flowing groundwater, the gel front may be torn apart and carried away as small particles of clay aggregates by the groundwater.

The strength of the gel front that will balance the shear force of the groundwater depends on the interactions of the clay aggregates. The most profound interaction of this concern is the edge-face electrostatic interaction among the clay particles. There still has been no reliable theoretical foundation for the strengths of such interactions. In this report we therefore will give a modelling approach based on experimental data of the Bingham¹ yield stress and the groundwater velocity in the fracture.

The model proposed in this report is similar to that of /Pusch 1983/ as has been discussed at the end of Section 2.1 of this report. We will, however, use a more straightforward approach to directly balance the Bingham yield stress of the gel front with the shear stress exerted on the front by the flow of the groundwater.

The Bingham yield stress of a clay depends on the ratio of clay solids and water in the clay body. It varies with the clay to water content ratio by a power-law relation. The yield stress depends also strongly on the salt content (or ionic strength) of the water. Some experimentally determined values of the Bingham yield stresses of different clay minerals are listed in Table 3-1.

Table 3-1. The Bingham yield stresses of different smectite minerals.

Mineral type	Clay/water wt. ratio (%)	Salt content (M)	Yield stress (Pa)	Ref.
Smectite-illite	8–13	0.001–0.02	18–120	/M'Bodj et al. 2004/
Na-montmorill	5–11	0.001–0.1	0.6–30	/Romos-Tejada et al. 2001/
Na-kaolinite	4.9–9.1	0.003–0.3	4–6	/Nickel 1997/
MX-80 benton.	2	Dist. water	< 0.1	/Pusch 1983/
	5		3	
	10		39	
	5	Allard water	3	
	10		28	
	20		~ 1,000	
	5	6·10 ⁻³ M NaCl	2	
	10		24	
	20		~ 900	
	5	3·10 ⁻³ M CaCl ₂	1	
	10		20	
	20		~ 750	
	5	6·10 ⁻² M NaCl	1	
	10		6	
	20		~ 300	
5	3·10 ⁻² M CaCl ₂	0.1		
10		0.5		
20		~ 20		

¹ A Bingham fluid acts like a solid when the shear stress is less than the yield stress. At higher stresses it acts like a fluid.

The data of the Bingham yield stress shown in Table 3-1 vary considerably for different smectite minerals, for different clay/water ratios as well as for different salt contents of the water. The values are especially sensitive to the clay/water ratio or water content in the clay. For our purpose the values for the MX-bentonite determined by /Pusch 1983/ are considered. The measured data of the rate of shear plotted against the shear stress for different water types at a clay/water ratio of 5% (wt.) are reproduced and shown in Figure 3-1. The yield stresses are obtained from the intersections with the horizontal axis of the extrapolated straight lines. These values are shown in Table 3-1, together with data obtained at other clay/water ratios by /Pusch 1983/. It is not clear how much the water content of the gel front in the fracture is, but it is unlikely to have clay/water weight ratios less than 5% /Pusch 1983/. Then the smallest value of the Bingham yield stress shown in the table for MX-bentonite is 1 Pa except for the case with a salt content of $3 \cdot 10^{-2}$ M CaCl_2 . Such high Ca^{2+} concentrations may not be representative of the pore water compositions, as has been shown by /Bruno et al. 1999/ that the cation-exchange reactions will result in Ca^{2+} concentrations in the pore water in the order of 10^{-3} M. In the following, we will use a yield stress value of 1 Pa which we deem is rather conservative for characterising the physical stability of the bentonite.

The shear force exerted by the flowing groundwater on the gel front will depend on the velocity of the groundwater at the clay-water interface in the intersecting fracture. The volumetric flowrate in a fracture can be calculated by the following equation:

$$Q = T \cdot W \cdot i$$

where Q is the volumetric flowrate ($\text{m}^3 \text{s}^{-1}$), T is the transmissivity of the fracture ($\text{m}^2 \text{s}^{-1}$), W is the width of the fracture (m), and i is the hydraulic gradient of the groundwater ($\text{mH}_2\text{O m}^{-1}$). The groundwater velocity in a fracture can be obtained by dividing Q with the cross section area of the fracture:

$$v = \frac{Q}{A} = \frac{Q}{W \cdot \delta} = \frac{T \cdot i}{\delta} \tag{3-1}$$

where v is the groundwater velocity (m s^{-1}) in the fracture, A is the cross-section area of the fracture (m^2), and δ is the aperture of the fracture (m).

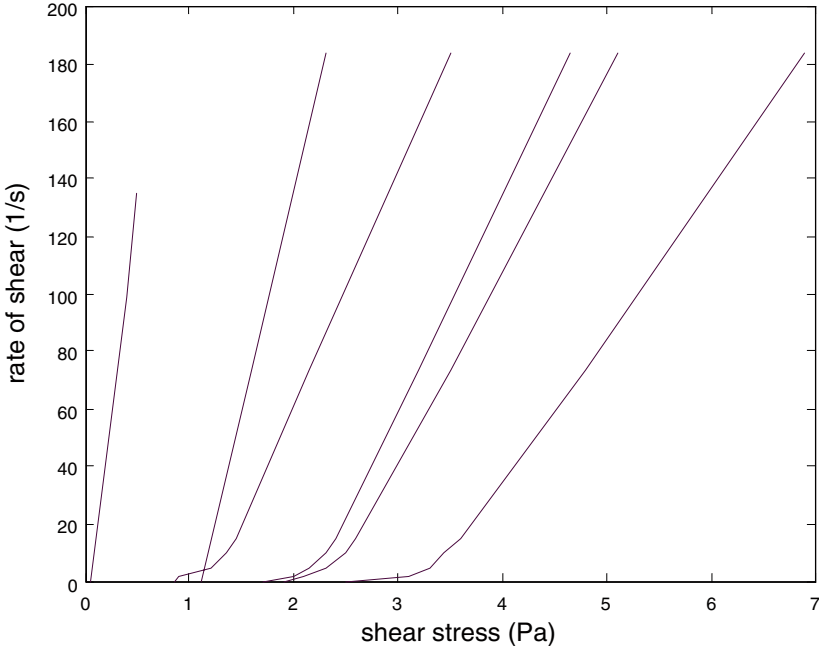


Figure 3-1. Rate of shear against shear stress of Na-bentonite measured by /Pusch 1983/. From left to right: the solutions used are $3 \cdot 10^{-2}$ M CaCl_2 , $6 \cdot 10^{-2}$ M NaCl , $3 \cdot 10^{-3}$ M CaCl_2 , $6 \cdot 10^{-3}$ M NaCl , Allard water, and distilled water, respectively. The clay/water ratio is 5% (wt.).

Typical values for the hydraulic gradient in the Swedish granitic rocks at repository depth are expected to be less than a few percent. Field measured data of transmissivity vary considerably but often between 10^{-6} and $10^{-9} \text{ m}^2 \text{ s}^{-1}$ /Andersson et al. 2002/. The fracture aperture may vary between less than a tenth of a millimetre and a few millimetres locally. Theoretically the transmissivity of a fracture should increase with the increase of fracture aperture, but fracture structures in granitic bedrocks are extremely heterogeneous and it is often difficult to give quantitative correlations between the transmissivity and the aperture of a fracture. In the following analyses, we will use a “central value” of 1%, i.e. $0.01 \text{ mH}_2\text{O m}^{-1}$, for the hydraulic gradient. For the transmissivity and fracture aperture, however, we will consider all combinations in the range of 10^{-6} to $10^{-9} \text{ m}^2 \text{ s}^{-1}$ for the transmissivity and 10^{-4} to $2 \cdot 10^{-3} \text{ m}$ (i.e. 0.1 to 2 mm) for the fracture aperture. The highest groundwater velocity in these ranges of transmissivity and fracture aperture will be 10^{-4} m s^{-1} and the lowest velocity will be $5 \cdot 10^{-9} \text{ m s}^{-1}$.

The shear stress of the groundwater exerted on the gel front can be calculated using Newton’s law of viscosity:

$$\tau_{yx} = -\eta \frac{dv_x}{dy} \quad (3-2)$$

where τ_{xy} is the shear stress (shear force per unit area) exerted on the gel front, η is the viscosity of water (10^{-3} Pa s), v_x is the groundwater velocity (m s^{-1}), and x and y are axis coordinates (m).

The results of the shear stress calculated by using Equations 3-1 and 3-2, and by taking dy to be on the order of the fracture aperture are shown in Figure 3-2. The choice of dy equal to the fracture aperture is based on the inspection of the physics giving rise to the velocity profile in a fracture. The friction between the fracture wall and flowing water generates a parabolic velocity profile over the aperture of the fracture. The velocity drops from the maximum in the centre of the fracture to zero at the wall over a distance of half the aperture. The presence of the gel will act similarly to the fracture wall and the effect on the velocity profile perpendicular to the gel will extend a similar distance.

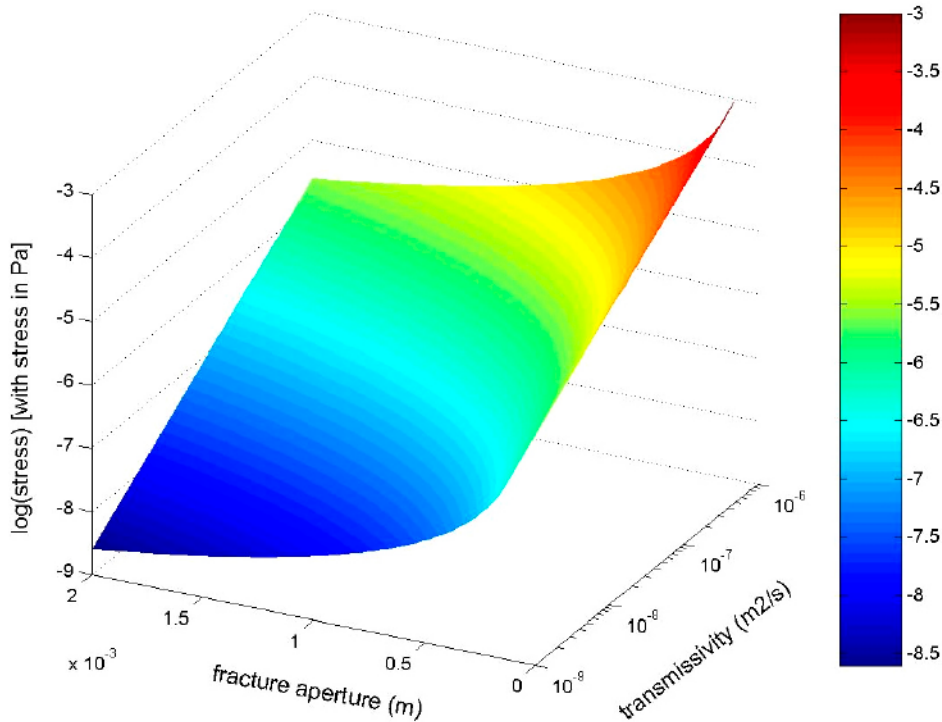


Figure 3-2. Shear stress on the front gel of bentonite exerted by the flowing groundwater in the intersecting fracture.

The results shown in Figure 3-2 indicate that, the highest shear stress will be 10^{-3} Pa when a fracture with the smallest aperture and the largest transmissivity (in the ranges we have considered) happens to intersect the deposition hole. The results also show that the shear stress exerted by the flowing groundwater is much less than the typical Bingham yield stress (1.0 Pa) of the gel front. It can thus be concluded that the bentonite buffer is physically stable with respect to the tearing off by the shear force exerted by the flowing groundwater on the gel front provided that the pore water does not have a very low ionic strength.

We will return to the question of the pore water chemistry at the outer rim of the clay when in contact with groundwater of very low ionic strength in the next section of this report.

In safety analyses of the spent fuel repository a climate scenario is often considered in addition to the base scenario /SKB 1999, 2004b, SKI 1996/. In the base scenario present-day climate conditions are assumed. In the climate scenario, possible dramatic changes of the future climate are also included. Historical climate change has been cyclical. During the Quaternary Period, i.e. the past 2 million years, the earth's climate has been characterised by global cold periods when continental ice sheets and glaciers have extended. The cold periods have been interrupted by shorter warm periods with a climate similar to the current. In the next 100,000 years, there will possibly be three glacial-interglacial cycles, with at least the largest glaciation to reach the entire Sweden /SKB 1999/. With the advance and retreat of the ice sheet, the earth's crust will be depressed and then up-lifted, the shoreline will rise and then sink. The hydraulic condition will be greatly influenced by the changes of hydraulic boundary conditions as a result of changed precipitation, shoreline displacement and ice growth and retreat /SKB 1999/. The hydraulic gradient of the deep groundwater will be increased profoundly when the ice sheet melts and recedes.

For our example calculations we take the hydraulic gradient as high as $1 \text{ mH}_2\text{O m}^{-1}$ and to last for a maximum of 100 years during the time that the ice recedes and the ice front passed the repository location. An idea of the duration of the extreme hydraulic gradient is useful to form an idea of whether possible high erosion rates must be studied in more detail.

We base these values on our interpretation of the description of the past ice ages and projection of future ice ages /SKB 1999/. From both Equations 3-1 and 3-2 it can be seen that the shear stress exerted by the flowing groundwater in the intersecting fracture on the gel front of the bentonite buffer is proportional to the hydraulic gradient. When the hydraulic gradient becomes 100 times larger in the climate scenario than in the base scenario (by assuming the current climate), the shear stress will be 100 times larger. The highest shear stress will then become 0.1 Pa. This is still less than the lower limit of the yield stress of the bentonite buffer that is about 1 Pa if it has an ion concentration above the CCC. When the large uncertainties (in the measured data of the yield stress, in the estimate of the hydraulic gradient and the fracture aperture) involved in this simple calculation are considered, the difference by a factor of 10 is deemed to be not large enough to conclude that the bentonite buffer is still physically stable against mechanical erosion during the time when the ice sheet recedes.

One approach is to assume that only the shear boundary layer, i.e. a distance of water, dy , will take up the clay particles at a concentration of the gel at the gel/water interface. In the sample calculations we use the value 5% by weight. This is the lowest figure reported by /Pusch 1983/ for the clay gels in waters with Ca somewhat higher than the CCC.

Loss of clay due to physical erosion will only occur when the shear stress at the gel/water interface is larger than the Bingham yield stress. This is expected to be on the order of 1 Pa.

The local shear stress can be estimated from

$$\tau_{yx} = -\eta \frac{dv_x}{dy} \cong -\eta \frac{v}{\delta} = -\eta \frac{Ti}{\delta^2} \quad (3-3)$$

Even for the highest values of the transmissivities T , gradients i and the lowest value of the fracture aperture δ , the shear stress is 0.1 Pa. Should for some reason the stress become larger than the Bingham yield stress the physical erosion rate can be roughly estimated by the following simple expression. It is based on the estimate that the gel is solubilised to a depth equal to the thickness of the shear boundary layer, see Equation 3-4. Similar results are obtained using an alternative model with the equivalent flowrate Q_{eq} for clay particles that diffuse out into the passing water.

$$N_{clay} = T \cdot i \cdot \delta \cdot c_{BentGel} \quad (3-4)$$

where N_{clay} is the rate of loss of clay due to erosion, $c_{BentGel}$ is the concentration of bentonite (kg m^{-3}) in the outermost layer of the gel. It is expected to be on the order of (some weight%) 10^3 's of kg m^{-3} . δ is the local fracture aperture.

For a transmissivity $T = 1 \cdot 10^{-6} \text{ m}^2 \text{ s}^{-1}$, a gradient $i = 1 \text{ mH}_2\text{O m}^{-1}$ and an aperture δ of 0.1 mm the rate of bentonite loss would be on the order of some tenths of kg a^{-1} . Note that this is based on the assumption that the shear stress is large enough to shear off gel, which was found previously not to be probable.

Another approach is to estimate the rate of diffusion from the solubilising gel boundary of the colloidal bentonite particles in the sol into the passing groundwater. These processes are described in the next section where the depletion of solutes (calcium) from the pore is described. The same formulae can be used for the colloidal clay particles. It will later be shown that this approach give erosion rates smaller than those just obtained above. However, the effects are additive.

4 Modelling of chemical stability of the bentonite

By the term “chemical stability” it is meant specifically the stability of the aggregates of the clay particles in the bentonite buffer. When the Na-montmorillonite in the bentonite buffer is in contact with water, clay gel may form. If the ionic strength of the water is lower than the critical coagulation concentration (CCC) of the Na-montmorillonite, the gel may disperse into a colloid sol in the water. The relatively abundant divalent cations, especially the Ca^{2+} , are of great importance since the CCC is inversely proportional to the square of the valence number (see Equation 2-1). For pure Na-montmorillonite, the clay will disperse readily in waters having concentrations lower than the CCC. When accessory minerals containing the cations of the CCC are present, dissolution of these minerals may buffer the concentration of the cations in the pore water of the clay to be higher than the CCC, and the dispersion of the clay to form colloid sols will then be determined by the mass transfer processes of the cations out of the pore water of the bentonite. In this report, we will consider only the calcium containing minerals (represented by gypsum or anhydrite) as a buffer of the calcium concentration in the pore water of the bentonite buffer. Other calcium containing minerals like calcite and siderite have solubilities lower than the CCC under the repository conditions and will not be considered in this report.

The mineral compositions of the two types of bentonite (the Wyoming type, MX-80, Na-bentonite and the Deponit CA-N type Ca-bentonite) are given in a Table in /SKB 2004b/. The table is reproduced below.

It should be noted that in this table the mineral compositions in the MX-80 bentonite is different from that in most previous works of SKB /e.g. Wanner et al. 1992, Wieland et al. 1994, Bruno et al. 1999/, e.g. the geochemical data of the MX-80 bentonite have also been given in /Bruno et al. 1999/:

Table 4-1. Bentonite composition of MX-80 and Deponit CA-N. The uncertainties are mainly related to the precision of the analysis method used.

Component	MX-80 (wt.%)	Deponit CA-N (wt.%)	Uncertainty (± wt.%)
Calcite+siderite	0	10	1
Quartz	3	1	0.5
Cristoballite	2	1	0.5
Pyrite	0.07	0.5	0.05
Mica	4	0	1
Gypsum	0.7	1.8 (anhydrite)	0.2
Albite	3	0	1
Dolomite	0	3	1
Montmorillonite	87	81	3
Na	72%	24%	5
Ca	18%	46%	5
Mg	8%	29%	5
K	2%	2%	1
Anorthoclase	0	2	1
CEC (meq/100g)	75	70	2
Organic carbon	0.2	0.2	–

Table 4-2. Geochemical data for MX-80 bentonite.

Property	Value	Reference
Cation exchange capacity (CEC)	85.0 meq/100g	/1/
Edge sites (OH groups)	2.8 meq/100g	/1/
Exchangeable Na	81.7%	/2/
Exchangeable Mg	3.9%	/2/
Exchangeable Ca	14.1%	/2/
Exchangeable K	0.3%	/2/
Total carbonate (CaCO ₃)	1.4 wt. %	/2/
Total quartz (SiO ₂)	10 wt. %	/3/
Total pyrite (FeS ₂)	0.3 wt. %	/8/
CaSO ₄ impurities	0.34 wt. %	/4/
NaCl impurities	0.007 wt. %	/4/
Plagioclase (mainly albite)	5 to 9 wt. %	/1, 5 and 6/
Illite	0 to 4 wt. %	/1 and 6/
Kaolinite	< 1 to 7 wt. %	/1 and 6/

In Table 4-2 it can be seen that the total carbonate content as CaCO₃ is assumed to be 1.4 wt.%. Moreover, 0.34 wt.% of gypsum/anhydrite (CaSO₄) has also been assumed.

4.1 Conceptual model

The conceptual model of the chemical stability of the bentonite buffer with respect to colloid dispersion we propose in this report can be described as follows:

After the closure of the repository, the bentonite buffer will be saturated by groundwater flowing in an intersecting fracture that is perpendicular to the axis of the canister. With water uptake, the bentonite will expand (intrude) somewhat into the fracture. The intrusion depth is assumed to be up to 15 cm, in accordance with the experimental and modelling results of /Pusch 1983/. We choose a large distance because this will give slightly conservative results.

The bentonite initially contains 0.7 wt.% of gypsum as is indicated in Table 4-1 for MX-80 bentonite. This figure is used only as an illustrative example. Other values could be readily used to substitute this figure when necessary. The bentonite is also assumed to have a bulk density of 2,100 kg m⁻³ (fully water saturated) and a porosity of about 40%. After saturation with groundwater, the pore water in the bentonite will have the equilibrium compositions calculated by /Bruno et al. 1999/ before the intrusion of glacial water. Of particular importance to our proposed model in this report are the Ca²⁺ concentrations in the pore water of the bentonite, 3.71·10⁻³, 2.04·10⁻³ or 1.96·10⁻³ M depending on the groundwater compositions (groundwaters at the Swedish Äspö, Finnsjön and Gideå sites, respectively).

The intrusion of glacial water during the period of ice sheet retreat will change the groundwater compositions in the fracture intersecting the deposition hole. The previous groundwater with relatively high salinity (e.g. the water at the Äspö site) will be replaced by the glacial water. The pore water inside the bentonite buffer will also be altered, approaching gradually the composition of the glacial water.

The groundwater flow and mass transfer processes considered in our model are the following (see Figure 4-1):

- Groundwater flows from the upstream, passing around the bentonite buffer that has expanded out into the fracture. The groundwater velocity is determined by the prevailing hydraulic gradient, the transmissivity and the (local) aperture of the fracture.

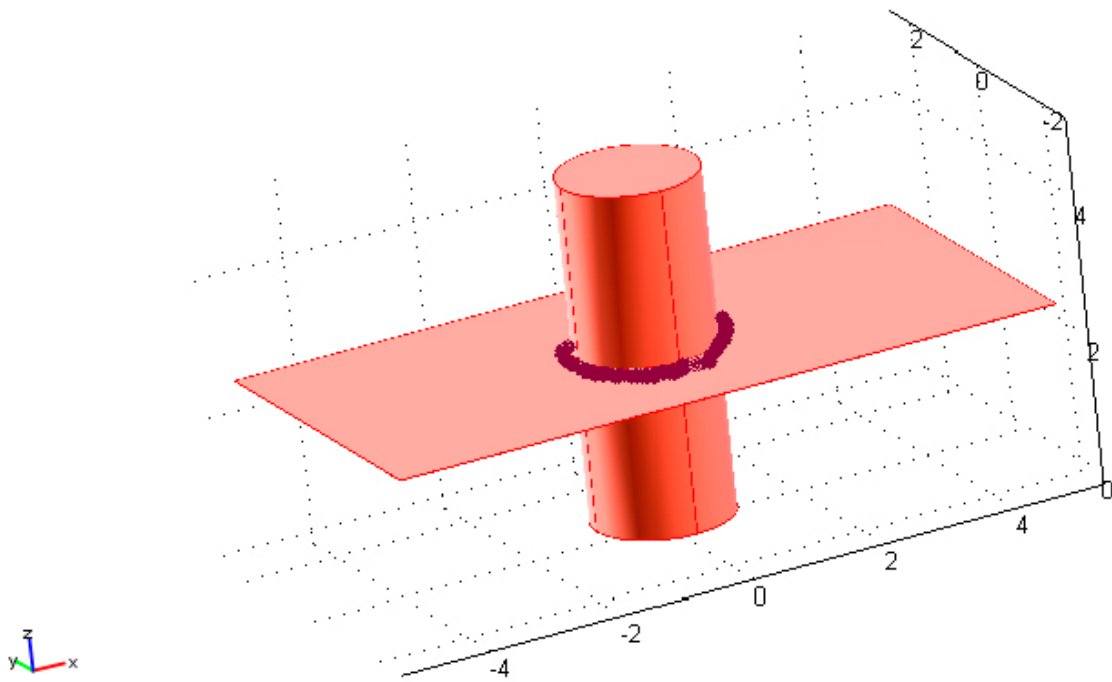


Figure 4-1. Geometrical arrangement of the intersecting fracture and the bentonite buffer and canister. The brown region surrounding the bentonite represents the intrusion into the fracture.

- The groundwater composition is assumed contain essentially no dissolved species, representing the downward penetration of the glacial melt water (an example of such groundwater composition can be the groundwater at the Swiss Grimsel site /Möri et al. 2003/.
- The pore water composition in the bentonite is assumed to have an initial equilibrium composition of the glacial water with the minerals (gypsum and calcite and pyrite) and cation-exchange sites of the bentonite. The aqueous species, especially the Ca^{2+} in the pore water of the bentonite, will diffuse from the bentonite into the passing groundwater. The rate of diffusion is determined by the concentration gradient built up in the bentonite (including the part of the intrusion in the fracture) and the advective flux in the flowing groundwater in the fracture. The groundwater carries away the calcium that has diffused out into it.

Different stages will be considered in our model. In an initial stage of glacial water intrusion, we assume that the bentonite, which had been equilibrated with typical saline groundwaters during the temperate period of a glaciation cycle, becomes equilibrated with typical fresh glacial groundwater, resulting in an initial concentration of the Ca^{2+} cations in the pore water of $9.8 \cdot 10^{-3}$ M in the gel at the gel/water interface. The fresh groundwater will flow in the fracture and Ca^{2+} will diffuse into the fresh water. The diffusive flux will form an upper-bound limit of the transport of Ca^{2+} into the water, since the concentration gradient of Ca^{2+} is now the largest.

This maximum rate of Ca^{2+} transport can then be estimated to give an upper-bound limit of the dissolution rate of the more soluble calcium mineral like gypsum. First for illustrative purposes we assume that when a parcel of clay has been depleted of gypsum and calcium in the pore water down to the CCC, the parcel will form a sol. Then by knowing the rate of depletion of calcium by diffusion to the passing water the rate of sol formation and loss of clay is obtained by assuming that the sol is carried away by the water. This gives an upper-bound limit of the clay colloid dispersion. This case of the initial stage dispersion will be presented in Section 4.2. This neglects a re-supply of calcium from the clay further from the interface to the water. It also neglects to account for any possible limitations in transport capacity of the clay particles by the water. If the clay sol cannot be fully carried away an additional diffusion resistance for calcium escape will build up and clay loss will decrease. This simple case is therefore conservative.

We then proceed to consider the intermediate stage when part of the bentonite intrusion in the fracture facing the flowing groundwater is depleted of gypsum and the calcium concentration in that part will drop to less than the solubility of gypsum. At the outmost region of the bentonite gel, the concentration may become equal to or lower than the critical coagulation concentration (CCC). The region of clay with calcium concentration less than CCC will disperse into the flowing groundwater. At this intermediate stage, however, we still assume that the loss of clay is moderate and the bentonite can still expand to fill the region of the lost clay, and therefore the depth of the bentonite intrusion into the fracture remains constant. This case of the intermediate stage dispersion will be considered in Section 4.3.

Should the loss of the clay become so massive that the bulk density of the bentonite buffer is noticeably lowered, the buffer could possibly lose some of its swelling capability. Then our assumption of constant depth of clay intrusion into the fracture will be not valid. However, the function indicator used in the safety analysis by SKB for the swelling pressure is $P_{swell} > 1 \text{ MPa}$ /SKB 2004/. To maintain such a swelling pressure, the buffer must have a bulk density $\rho_{bulk} > 1,550\text{--}1,900 \text{ kg m}^3$ /SKB 2004a/. Moreover, to safely exclude microbial activity (which is especially detrimental to copper canister corrosion by reduction of the abundant sulphate in the groundwater to sulphide), we must have $\rho_{bulk} > 1,800 \text{ kg m}^3$ /SKB 2004/. These requirements imply that, before the bentonite considerably loses its swelling pressure, its other function indicators may have already been violated. With all these issues in mind, we will therefore in this report not proceed to the late stages of clay colloid dispersion when the bentonite buffer loses its swelling pressure. Consequently in our following models it is legitimate to assume a constant geometry of the bentonite buffer, i.e. a constant radius of the bentonite proper in the disposition hole and a constant depth of the intrusion of the buffer into the intersecting fracture.

4.2 The upper-bound limit calculation of the initial release rate of calcium

The initial release of calcium depends on the solubility of the gypsum in the bentonite and the groundwater flow velocity in the intersecting fracture. A central value of $9.8 \cdot 10^{-3} \text{ M}$ of gypsum solubility will be used in the following calculations (see discussions in the Section 4.1). The groundwater velocity is determined by the hydraulic gradient of the groundwater, the transmissivity and the aperture of the fracture. All of them vary considerably in deep crystalline rocks. For illustrative purposes we will first present a calculation using some representative “central values” of the hydraulic gradient, the transmissivity and aperture of the fracture. The values are $0.01 \text{ mH}_2\text{O m}^{-1}$ for the hydraulic gradient, $10^{-8} \text{ m}^2 \text{ s}^{-1}$ for the transmissivity and 10^{-4} m for the fracture aperture.

The model used for the calculation is two-dimensional. The intersecting fracture is modelled as a 2-dimensional domain (see Figure 4-1). The outer periphery of the intruding bentonite is assumed to be a circular boundary with a radius of 1 m. This figure represents the sum of the radii of the copper canister (0.5 m), the thickness of the bentonite buffer (0.35 m) and the intrusion depth of the bentonite (0.15 m). The other boundaries are the inflow boundary and the outflow boundary, as well as the boundaries of symmetry parallel to the flow direction. The diffusive transport is coupled with the groundwater flow and is modelled by assigning a constant concentration of 9.8 mM at the boundary of the circle. The coupled multiphysical problem is solved by the FEMLAB program /Comsol 2004/. The concentration profile and the velocity arrows are shown in Figure 4-2.

The integrated total flux of calcium along the boundary of the outer periphery of the intruding bentonite is $1.49 \cdot 10^{-10} \text{ mol s}^{-1}$ (or $4.68 \cdot 10^{-3} \text{ mol a}^{-1}$) for this special case. The equivalent flowrate (see discussions below) Q_{eq} is $4.78 \cdot 10^{-4} \text{ m}^3 \text{ a}^{-1}$. When the gypsum content in the bentonite buffer is assumed to be 0.7 wt.% and a solid/water ratio to be 4.85 kg L^{-1} , the above integrated total flux of calcium gives a rate of bentonite loss of 112 g a^{-1} .

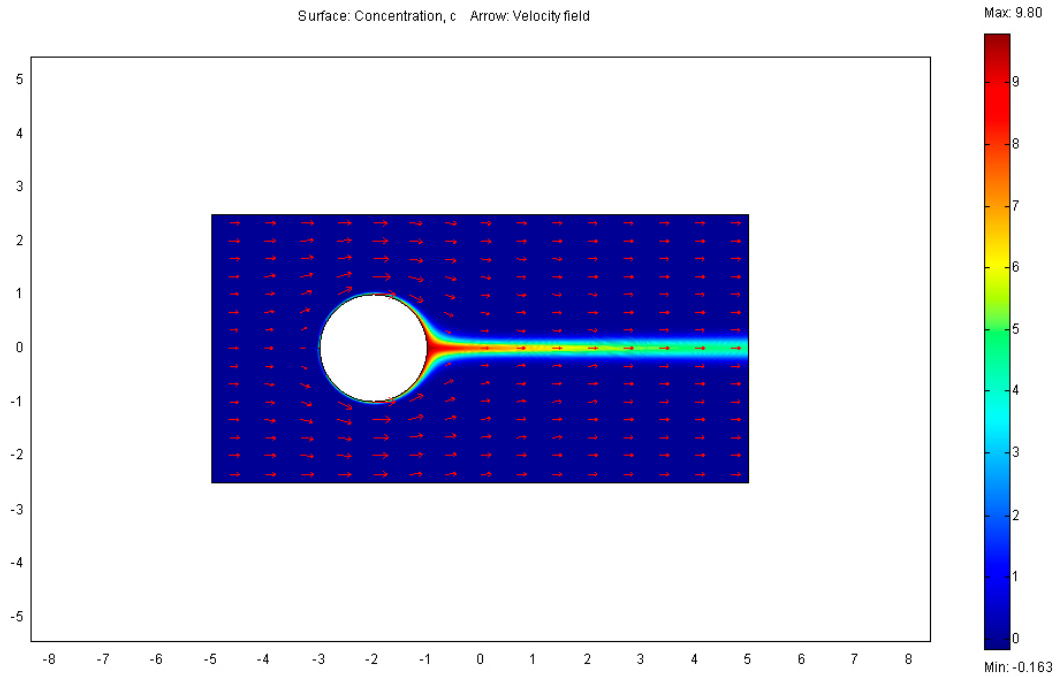


Figure 4-2. Groundwater flows in the intersecting fracture and surrounding the canister. Calcium is transported from the surface of the gel front into the groundwater. The calcium concentration profile is shown by the colour surface plot and the groundwater velocity by the arrow plot.

The various input data used in the above calculation are summarised in the following table.

In the above calculation, both the transmissivity and the aperture of the fracture have been assigned central values. These two parameters are known to vary over very large ranges. In the following we will make calculations using ranges of the values as shown in Table 4-3.

Alternatively, the diffusive flux of the calcium from the outer periphery of the bentonite intrusion will be calculated by the product of an equivalent flowrate, Q_{eq} , and the difference between the boundary concentration and the concentration in the approaching groundwater, the latter in our case is assumed to be zero. The equivalent flowrate is a very illustrative entity which shows what flowrate would carry away the species with the concentration it has at the clay boundary if the approaching concentration of the water is zero. If it is not it is defined by Equation 4-1.

$$N = Q_{eq} (c_0 - c_w) \quad (4-1)$$

where N (mol s^{-1}) is the rate of loss of the calcium from the outer surface of the bentonite intrusion into the groundwater, Q_{eq} ($\text{m}^3 \text{s}^{-1}$) is the equivalent flowrate, and c_0 and c_w (mol m^{-3}) are calcium concentrations at the outer surface and in the groundwater, respectively.

Table 4-3. Input data used in the upper-bound calculations.

Property	Value
Transmissivity of the fracture	$1 \cdot 10^{-8} \text{ m}^2 \text{ s}^{-1}$ ($1 \cdot 10^{-9}$ to $1 \cdot 10^{-6} \text{ m}^2 \text{ s}^{-1}$)*
Aperture of the fracture	$1 \cdot 10^{-4} \text{ m}$ ($1 \cdot 10^{-4}$ to $2 \cdot 10^{-3} \text{ m}$)*
Outer radius of bentonite including the intrusion in fracture	1 m
Hydraulic gradient of the groundwater	0.01 $\text{mH}_2\text{O m}^{-1}$
Gypsum content in bentonite	0.7 wt.%
Diffusivity of Ca in water	$D_w = 1 \cdot 10^{-9} \text{ m}^2 \text{ s}^{-1}$
Solubility of gypsum	9.8 mol m^{-3} (9.8 mM)

* The ranges of values will be used in the following calculations.

The equivalent flowrate for the specific geometry considered in this report will be given by /Neretnieks 1982, Nilsson et al. 1991, Nordman and Vieno 2004/:

$$Q_{eq} = 2\pi r \delta \sqrt{\frac{4D_w v}{\pi^2 r}} = 4\delta \sqrt{D_w r v} = 4\sqrt{D_w r T i \delta} \quad (4-2)$$

where r (m) is the radius of the out periphery of the bentonite intrusion, δ (m) is the fracture aperture, D_w ($\text{m}^2 \text{s}^{-1}$) is the diffusivity of a solute (calcium) in water, and v (m s^{-1}) is the groundwater velocity. The groundwater velocity is related to the hydraulic gradient, the transmissivity and aperture of the fracture by Equation 3-1. The use of Equation 4-2 obviates the need to numerically solve the flow and diffusion equations as was done to generate Figure 4-2 for every parameter combination.

The equivalent flowrate is calculated by using the data listed in Table 4-3 (the ranges of values for the fracture transmissivity and fracture aperture are used). The results are shown in Figure 4-3.

The calculated equivalent flowrate ranges from $1.26 \cdot 10^{-4} \text{ m}^3 \text{ a}^{-1}$ when the transmissivity is $1 \cdot 10^{-9} \text{ m}^2 \text{ s}^{-1}$ and the fracture aperture is $1 \cdot 10^{-4} \text{ m}$, to $1.78 \cdot 10^{-2} \text{ m}^3 \text{ a}^{-1}$ when the transmissivity is $1 \cdot 10^{-6} \text{ m}^2 \text{ s}^{-1}$ and the fracture aperture is $2 \cdot 10^{-3} \text{ m}$. Using the solubility of gypsum for c_0 the release rate of calcium will then be $1.23 \cdot 10^{-3} \text{ mol a}^{-1}$ and $1.77 \cdot 10^{-1} \text{ mol a}^{-1}$ respectively. The corresponding losses of bentonite when assuming a gypsum content of 0.7 wt.% are $2.95 \cdot 10^{-2} \text{ kg a}^{-1}$ and 4.25 kg a^{-1} respectively. These two results are summarised in Table 4-4.

It should be noted that the results of the approach with the concept of equivalent flowrate agree well with those obtained by the detailed coupled mass transport and flow modelling using the FEMLAB program. For the case that has been calculated using FEMLAB with the fracture transmissivity of $1 \cdot 10^{-8} \text{ m}^2 \text{ s}^{-1}$ and the fracture aperture of $1 \cdot 10^{-4} \text{ m}$, the fully coupled approach gives an equivalent flowrate, Q_{eq} , of $4.78 \cdot 10^{-4} \text{ m}^3 \text{ a}^{-1}$. When Q_{eq} is calculated using Equations 4-1 and 4-2 with the concept of equivalent flowrate, the value of Q_{eq} will be $3.98 \cdot 10^{-4} \text{ m}^3 \text{ s}^{-1}$. Therefore in the following model calculations of this report, we will mainly use the approach of the equivalent flowrate.

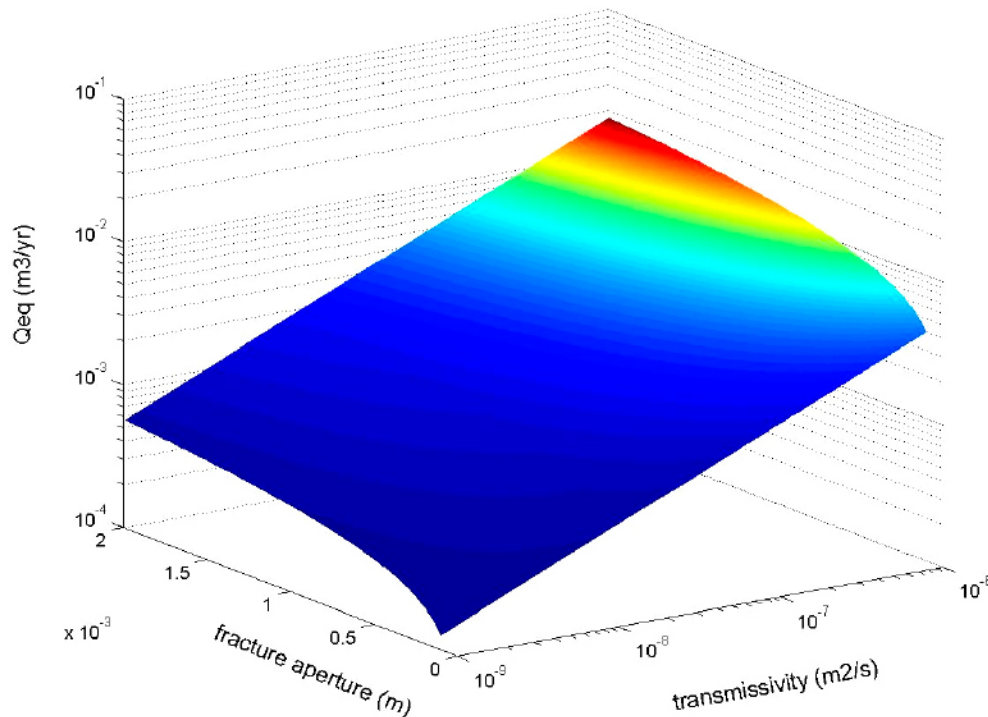


Figure 4-3. Equivalent flowrate calculated by using the data shown in Table 4-3.

Table 4-4. The ranges of fracture transmissivity and fracture aperture, the equivalent flowrate, and the results of the rate of calcium loss and bentonite loss at the initial stage.

Property	Low value	High value
Transmissivity of the fracture	$1 \cdot 10^{-9} \text{ m}^2 \text{ s}^{-1}$	$1 \cdot 10^{-6} \text{ m}^2 \text{ s}^{-1}$
Aperture of the fracture	$1 \cdot 10^{-4} \text{ m}$	$2 \cdot 10^{-3} \text{ m}$
Equivalent flowrate	$1.26 \cdot 10^{-4} \text{ m}^3 \text{ a}^{-1}$	$1.78 \cdot 10^{-2} \text{ m}^3 \text{ a}^{-1}$
Rate of calcium loss	$1.23 \cdot 10^{-3} \text{ mol a}^{-1}$	$1.74 \cdot 10^{-1} \text{ mol a}^{-1}$
Rate of bentonite loss	$2.95 \cdot 10^{-2} \text{ kg a}^{-1}$	4.19 kg a^{-1}

When the radius of the copper canister is taken to be 0.5 m, the thickness of the bentonite buffer 0.35 m, and the length of the copper canister 5 m, the volume of the annulus of the bentonite buffer will be 7.4 m^3 . Further by assuming a bulk density of the buffer to be $2,100 \text{ kg m}^{-3}$ and a porosity of 40%, the dry density of the buffer will be $1,700 \text{ kg m}^{-3}$. The total mass of the bentonite buffer will then be $1.26 \cdot 10^4 \text{ kg}$. Should the initial rate of calcium loss remain constant at later stages of calcium loss (this is not the case as will be discussed in the next subsection), and the high value of the rate of calcium loss in Table 4-3 be used, the entire bentonite buffer in a repository will be lost within $2.96 \cdot 10^3$ years. Note also that these results apply for a very fresh water approaching the canister and calcium concentration equal to the solubility of gypsum. After some time the calcium concentration at the bentonite water interface will decrease as the dissolution front of gypsum recedes into the bentonite.

Further elaboration of the chemical stability will not be pursued here since what we have modelled here is just the very initial stage of the bentonite loss. More detailed discussions will be provided in the next subsection.

4.3 Modelling bentonite loss after the initial period

In the previous subsection, we studied the initial stage of the loss of calcium and bentonite. The initial stage will last during a period during which pseudo steady condition for the chemical gradients and the intrusion rate of the clay is established. It is estimated to be less than a few years.

The subsequent mass transport of calcium will be different from the initial stage. In this report the groundwater flowing in the intersecting fracture is assumed to be essentially fresh water with zero concentration of calcium (and other species as well). When calcium is released from the outer periphery of the gel front of the bentonite into the fresh groundwater, the concentration of calcium in the pore water in the gel front will start to decrease. When the pore water concentration in the bentonite becomes lower than the solubility of gypsum, the gypsum mineral will dissolve. In the region where the gypsum has been depleted, the pore water concentration will no longer be equal to the solubility of gypsum but be lower than that. Furthermore, at the outer edge of the gel front, the calcium concentration in the pore water may become less than the critical coagulation concentration (CCC) of the bentonite clay, and the clay at the outer edge of the gel front will be dispersed to clay sols that will be carried away by the groundwater. As has been discussed in the previous subsection, we still assume that the loss of clay is moderate and the bentonite can still expand to fill the region of the loss clay, and therefore the depth of the bentonite intrusion into the fracture remains constant.

The following conceptualisations are used to set up the model of the intermediate stage of bentonite clay dispersion.

The clay in the deposition hole has a swelling pressure that acts as a force to push out the clay into the fracture. As the clay moves out into the fracture it expands and the swelling pressure decreases with decreasing clay density. During swelling the clay takes up water and equilibrates

with the local water composition. There will therefore be a gradient of water content as well as of the water chemistry along the swollen clay. A final state is eventually approached when the friction force of the clay against the walls of the fracture balances the force that pushes the clay out into the fracture. At the outer rim of the clay the clay forms a stable gel and no particles are carried away if the salt concentration is above the CCC.

Next, let the water composition at the outer edge of the clay change so that it will be lower than the CCC. For simplicity of description we assume that it is the calcium concentration in the water that determines the CCC. Also consider a case where there is a constant exchange of water with a known rate Q_{eq} with an approaching concentration c_w that is assumed to be zero in this report. When the pore water has a higher concentration of calcium than the water outside the clay, calcium diffuses out from the gel to the water. The water will take up calcium at the outer rim of the bentonite gel and leave with a concentration c_i .

At some point in the gel the calcium concentration would become less than CCC. The clay particles will disperse and be carried away by the water. This implies that the concentration at the gel/sol interface will be equal to the CCC. This will also be the concentration in the leaving water. Thus $c_i = CCC$.

This of course is a simplified model because in the fracture the approaching water will first meet clay that gives off calcium, which has to diffuse out further in the water in the fracture. It will therefore develop a concentration gradient in the water that passes the clay and the longer the water has been in contact with clay the further out the calcium has diffused. This can be handled by the boundary layer theory and has previously been used to describe the transport to and from the clay at the fracture interface. On the average the transport capacity of the flowing water can be summarized in an equivalent flowrate Q_{eq} ($m^3 a^{-1}$). This is the flowrate of water that will carry away the calcium with a concentration equal to that at the interface, c_i minus that in the approaching water c_w . The equivalent flowrate is given by Equations 4-1 and 4-2.

As calcium is transported into the groundwater, the gypsum mineral inside the bentonite buffer dissolves. Somewhere inside the gel intrusion and from there to the gel rim facing the groundwater, the gypsum has been completely depleted. In this region, the calcium concentration in the pore water drops from the solubility of gypsum, c_s , to c_i at the gel rim (see Figure 4-4). In the region where the gypsum mineral has not been depleted, the calcium concentration in the pore water will be equal to the solubility of gypsum. The calcium in the pore water is first transported from the front of the gypsum mineral to the outer rim of the bentonite gel, and is then transported into the groundwater from the gel surface. We assume that a steady state will prevail so that the thickness of the clay intrusion in which the clay still contains gypsum and the thickness in which the clay is depleted of gypsum are both constant. The validity of the constant geometry assumption has been discussed earlier.

The flux of calcium transported from the outer rim of the bentonite gel into the groundwater is still described by Equations 4-1 and 4-2. The concentration c_0 in Equation 4-1, however, has to be replaced by c_i , i.e. instead of using the solubility of gypsum we now use the CCC of the bentonite clay. When the flow properties are assumed to be the same as in the previous subsection, Q_{eq} will be exactly the same. As the CCC is assumed to be 1 mM and the solubility, c_s , 9.8 mM, the rate of calcium loss as well as the rate of bentonite loss will just be 9.8 times less than the rates we have calculated in the previous subsection. The results of the rate of calcium loss and the rate of bentonite loss at the intermediate stage are shown in Table 4-5.

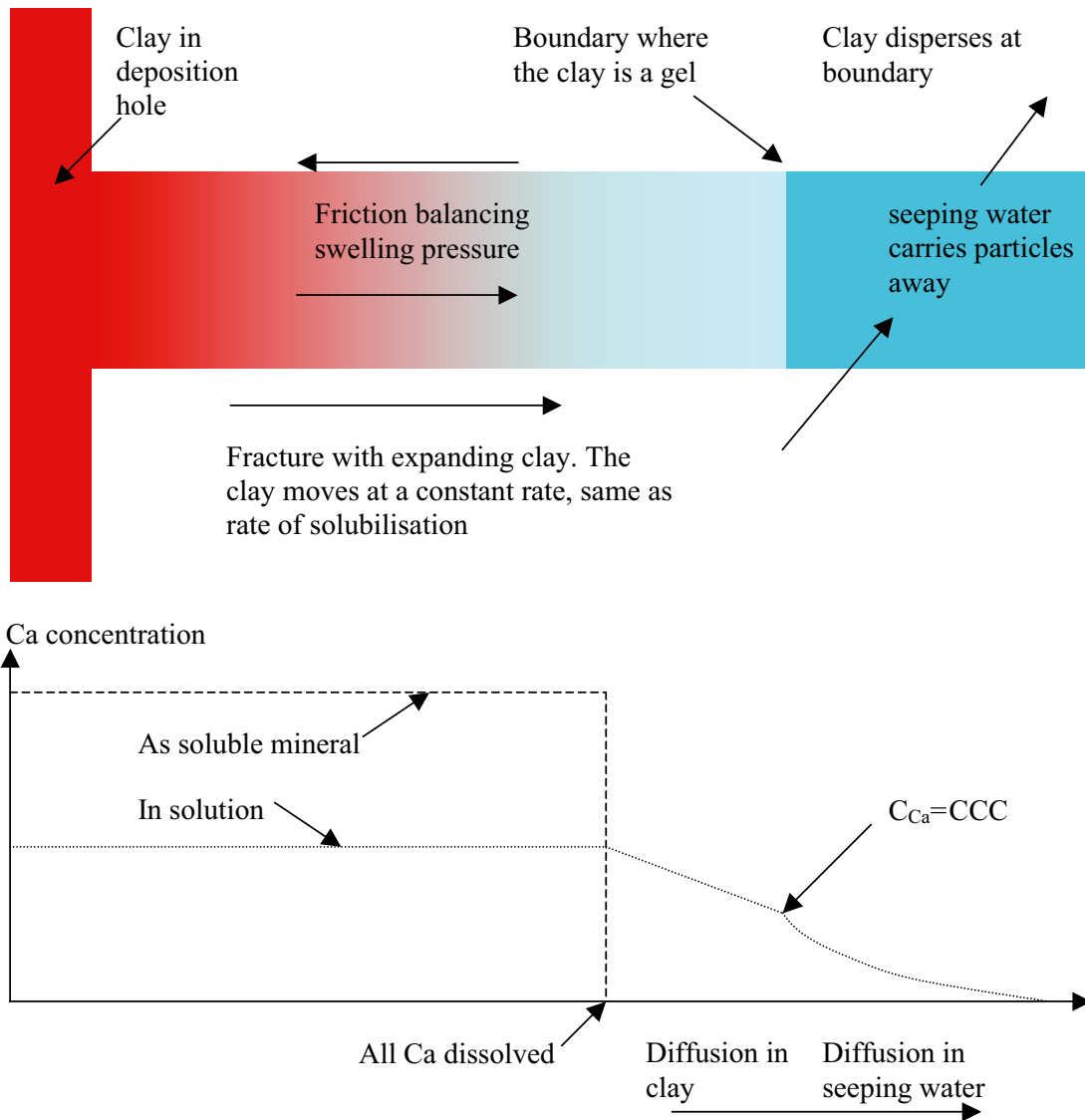


Figure 4-4. Clay swells into a fracture. The Ca minerals dissolve and Ca diffuses towards the flowing groundwater water. Ca concentration drops to CCC. Clay disperses into the groundwater and is carried away by the water.

Table 4-5. The ranges of fracture transmissivity and fracture aperture, the equivalent flowrate, and the results of the rate of calcium loss and bentonite loss at the intermediate stage.

Property	Low value	High value
Transmissivity of the fracture	$1 \cdot 10^{-9} \text{ m}^2 \text{ s}^{-1}$	$1 \cdot 10^{-6} \text{ m}^2 \text{ s}^{-1}$
Aperture of the fracture	$1 \cdot 10^{-4} \text{ m}$	$2 \cdot 10^{-3} \text{ m}$
Equivalent flowrate	$1.26 \cdot 10^{-4} \text{ m}^3 \text{ a}^{-1}$	$1.78 \cdot 10^{-2} \text{ m}^3 \text{ a}^{-1}$
Rate of calcium loss	$1.26 \cdot 10^{-4} \text{ mol a}^{-1}$	$1.78 \cdot 10^{-2} \text{ mol a}^{-1}$
Rate of bentonite loss when bentonite contains gypsum	$3.0 \cdot 10^{-3} \text{ kg a}^{-1}$	0.43 kg a^{-1}
Rate of bentonite loss if there is no gypsum in bentonite	0.536 kg a^{-1}	76.9 kg a^{-1}

The values in the last row of the table are obtained by assuming that the bentonite does not contain gypsum or other calcium minerals, and the calcium concentration in the pore water of the bentonite is just that of CCC.

In the above discussions we assumed that the gypsum dissolution front (the demarcation line between the region where the gypsum has not been depleted and where it has been) lies in the intrusion zone in the intersecting fracture rather than in the bentonite proper inside the deposition hole. We will in the following show that from a transport resistance point of view this is the case for the flow and transport conditions considered in this report.

As is shown in Figure 4-4, the radius of the gel rim (measured from the central axis of the canister) where the calcium concentration is CCC is $b = 1$ m. Assume that the radius of the gypsum dissolution front is a (m). Then the rate of calcium transport from a to b is

$$r = \frac{2\pi D_B (c_0 - c_i) \delta}{\ln(b/a)} \quad (4-3)$$

At steady state it should equal to the rate of transport of calcium from the gel rim to the groundwater.

$$\frac{2\pi D_B (c_0 - c_i) \delta}{\ln(b/a)} = Q_{eq} (c_i - c_w) \quad (4-4)$$

where D_B ($1 \cdot 10^{-11} \text{ m}^2 \text{ s}^{-1}$) is the diffusivity of calcium in the pore water in bentonite, c_0 (9.8 mol m^{-3}) is the solubility concentration of the gypsum mineral, c_i (1.0 mol m^{-3}) is the CCC, δ (m) is the fracture aperture, b (1.0 m) is the radius of the outer rim of the bentonite gel, a (m) is the radius of the gypsum dissolution front, Q_{eq} ($\text{m}^3 \text{ s}^{-1}$) is the equivalent flowrate, and c_w (0 mol m^{-3}) is the calcium concentration in the groundwater.

After inserting Equations 4-1 and 4-2 into Equation 4-4, we get

$$\ln a = \ln b - \frac{\pi D_B (c_0 - c_i) \sqrt{\delta}}{2\sqrt{D_w T i b} (c_i - c_w)} \quad (4-5)$$

where D_w ($1 \cdot 10^{-9} \text{ m}^2 \text{ s}^{-1}$) is the diffusivity of calcium in water, T ($\text{m}^2 \text{ s}^{-1}$) is the transmissivity of the fracture, and i ($0.01 \text{ mH}_2\text{O m}^{-1}$) is the hydraulic gradient of the groundwater.

It can be seen from Equation 4-5 that a will be smallest when δ is the largest and T is the smallest. In the ranges of values we have considered for them, the largest δ and the smallest T are $2 \cdot 10^{-3} \text{ m}$ and $1 \cdot 10^{-9} \text{ m}^2 \text{ s}^{-1}$ respectively. When these values together with the values for the other parameters given above are used, the value of a is 0.94 m. This implies that inside the 0.15 m-thick bentonite intruded into the fracture, 0.06 m has been depleted of the gypsum mineral, and the gypsum dissolution front lies in the region of bentonite intrusion in the fracture.

Even in the case when the gypsum dissolution front does not lie inside the bentonite intrusion in the fracture but in the bentonite proper in the deposition hole, our above modelling approach will still be valid for steady state conditions. The rate of calcium loss into the groundwater is determined only by the equivalent flowrate of the groundwater, Q_{eq} , and the difference between calcium concentrations at the outer gel rim (c_i) and in the groundwater (c_w). None of these parameters are influenced by the transport of calcium inside the bentonite. We have not considered the balance of friction forces and swelling pressure in this analysis and just assumed that loss of clay by solubilisation can be replenished from the deposition hole.

In the following we will analyse the consequences of the steady-state, intermediate-stage release of calcium.

In safety assessment of spent fuel repository, several function indicators of the bentonite buffer are given by its bulk density /SKB 2004/. When the bentonite is lost by dispersion to clay sols, the bulk density of the bentonite will decrease. Assume a mass of m kg of bentonite is lost, the bulk density becomes

$$\rho_{bulk} = \rho_{bulk}^0 - \frac{m}{V} \left(1 - \frac{\rho_w}{\rho_{dry}}\right) \quad (4-6)$$

where ρ_{bulk} (kg m^{-3}) is the bulk density of the bentonite ρ_{bulk}^0 after losing m (kg) of bentonite, ρ_{bulk}^0 ($2,100 \text{ kg m}^{-3}$) is the original bulk density of bentonite, ρ_w ($1,000 \text{ kg m}^{-3}$) is the density of water ρ_{dry} , ($1,700 \text{ kg m}^{-3}$) is the dry density of bentonite, and V (7.4 m^3) is the total volume of bentonite in one deposition hole.

The changes of bulk density of bentonite with time are plotted in Figure 4-5 using the different rates of bentonite loss shown in the last two rows in Table 4-4.

It can be seen from the results that, when the bentonite contains 0.7 wt.% of gypsum, the bulk density will drop to $1,500 \text{ kg m}^{-3}$ after about $3 \cdot 10^4$ years in contact with fresh groundwater if the transmissivity and aperture of the intersecting fracture are large (the green line); if they are small, the bulk density will drop to about $1,930 \text{ kg m}^{-3}$ after 10^6 years (the blue line). On the other hand, when the bentonite does not contain gypsum, the bulk density will drop to $1,500 \text{ kg m}^{-3}$ after about 150 years if the transmissivity and aperture of the fracture are large (the black line); if they are small, the bulk density drops to $1,500 \text{ kg m}^{-3}$ after about $2 \cdot 10^4$ years in contact with fresh groundwater (the red line).

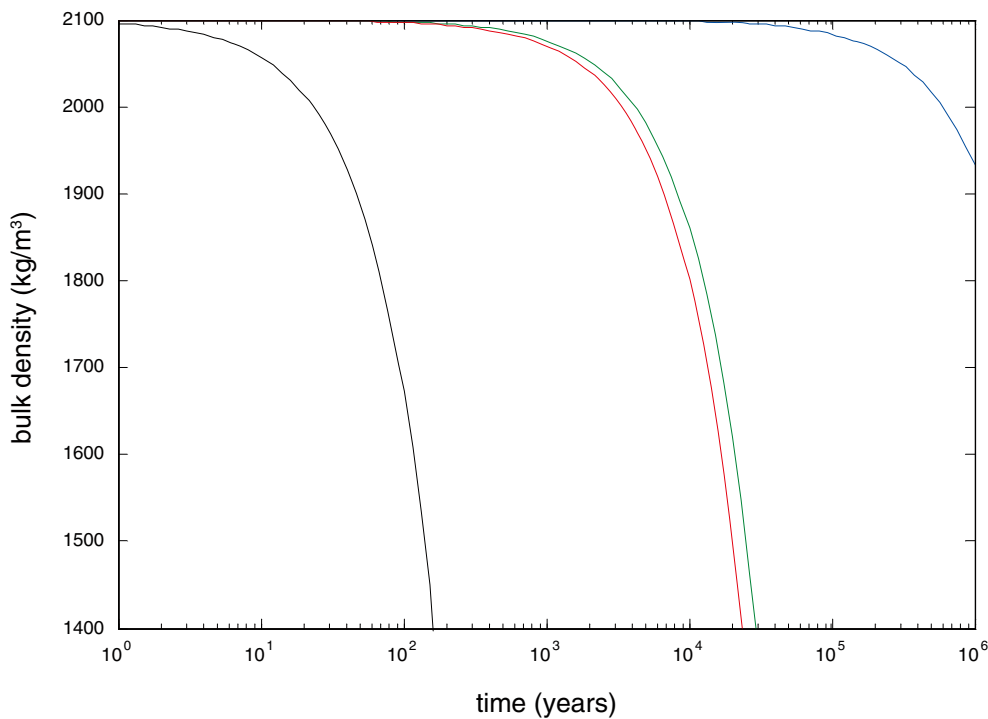


Figure 4-5. Changes of the bulk density with time with different rates of bentonite loss shown in the last two rows of Table 4-4. The blue line: low values of the transmissivity and fracture aperture, and the bentonite contains 0.7 wt.% gypsum. The green line: high values of the transmissivity and fracture aperture, and the bentonite contains 0.7 wt.% gypsum. The red line: low values of the transmissivity and fracture aperture, and the bentonite does not contain gypsum. The black line: high values of the transmissivity and fracture aperture, and the bentonite does not contain gypsum.

Fresh water from melting ice might intrude to repository depth during an ice age. During some periods a considerably higher hydraulic gradient and water flowrate can be expected. The water may then not have time to dissolve much minerals and can have much lower calcium content than otherwise. In order to form some idea of the possible duration of fresh water intrusion we consider the following. Note, however, that this section is not meant to be any prediction. It is useful when developing models to assess what time range of validity they could be expected to have.

The length of time during which the bentonite buffer is in contact with fresh groundwater depends on the duration of the ice-sheet cover during a glacial/interglacial cycle. This in turn depends on the geographical location of the site of the repository. In Sweden, the Bberg area (the Finnsjön area in central Sweden) will be infiltrated by fresh water during 74,000 of the 130,000 years of the next glacial/interglacial cycle, i.e. about 56.9% of the total time. In the Cberg area (the Gideå area also in central Sweden, but to the north of the Bberg), the fresh water infiltration time will be 84,000 years out of the total 130,000 years (64.6%) /SKB 1999/. If all the future glacial cycles are expected to be similar, the above argument implies that during more than half of the future time the repository site could be infiltrated by fresh groundwater and that the bentonite buffer will be in contact with the fresh water. The bulk density of bentonite will drop to less than $1,500 \text{ kg m}^{-3}$ (and thus all of its function indicators are violated) in less than $3 \cdot 10^4$ years except for the case when the bentonite contains 0.7 wt.% of gypsum and when the transmissivity and aperture of the fracture are small in the range of values we have considered. In the latter case the bulk density will drop to about $1,930 \text{ kg m}^{-3}$ after 10^6 years.

However, when the ice recedes and there is a thick ice cover at one line but ice has melted away on the other side of the line, high hydraulic gradients can develop in the rock under the melting ice front.

If we, for illustrative purposes, assume that the gradient is as high as $1 \text{ mH}_2\text{O m}^{-1}$ at the repository location while the ice recedes the equivalent flowrate Q_{eq} will be 10 times higher than the values shown earlier for the same transmissivity and aperture. This high gradient is not deemed to last over very long times, however.

5 Summary of the models

In the previous sections we have developed the models for bentonite loss due to physical and chemical erosion. Sample calculations were made using values of the main parameters that were deemed to be within the ranges that can be expected for Swedish sites and the bentonites that have been suggested for use as buffer materials.

5.1 Physical erosion

It was found that physical erosion could possibly occur only under the highest hydraulic gradients and in the most conductive fractures.

Loss of clay due to physical erosion will only occur when the shear stress at the gel/water interface is larger than the Bingham yield stress. This is expected to be on the order of 1 Pa.

The local shear stress can be estimated from Equation 3-2 given earlier:

$$\tau_{yx} = -\eta \frac{dv_x}{dy} \cong -\eta \frac{v}{\delta} = -\eta \frac{Ti}{\delta^2} \quad (5-1)$$

Even for the highest values of the transmissivities T , the hydraulic gradients i and the lowest value of the fracture aperture δ , the shear stress is 0.1 Pa. Should for some reason the stress become larger than the Bingham yield stress the physical erosion rate can be roughly estimated by the following simple expression. It is based on the estimate that the gel is solubilised to a depth equal to the thickness of the shear boundary layer, see Equation 5-2. Similar results are obtained using an alternative model using the equivalent flowrate Q_{eq} for clay particles that diffuse out into the passing water.

$$N_{clay} = T \cdot i \cdot \delta \cdot c_{BentGel} \quad (5-2)$$

where N_{clay} is the rate of loss of clay due to erosion (kg s^{-1}), $c_{BentGel}$ is the concentration of bentonite (kg m^{-3}) in the outermost layer of the gel. It is expected to be on the order of (some weight%) 10's of kg m^{-3} . δ is the local fracture aperture.

For a transmissivity $T = 1 \cdot 10^{-6} \text{ m}^2 \text{ s}^{-1}$, a hydraulic gradient $i = 1 \text{ mH}_2\text{O m}^{-1}$ and an aperture δ of 0.1 mm the rate of bentonite loss would be on the order of some hundreds of grams per year.

5.2 Chemical erosion

As long as the pore water in the bentonite has a concentration of divalent ions (calcium) in excess of the CCC the loss of bentonite due to sol formation at the bentonite/water interface will be determined by the rate of loss of calcium from the clay. Then the amount of clay that has had its pore water depleted of the calcium can be solubilised and carried away by the water.

When there are minerals still present that replenish the pore water with divalent ions such as calcium to a concentration exceeding the CCC, calcium can be lost without clay being solubilised. When the calcium mineral has been depleted in the region nearest the gel/water interface a balance will be established between the rate of replenishment of the calcium by diffusion from where there is still calcium mineral and the rate of loss of calcium at the gel/water interface. The rate of loss of calcium can then be calculated from

$$N_{Ca} = Q_{eq}(C_{CCC} - c_w) \quad (5-3)$$

and the rate of loss of clay is:

$$N_{clay} = \frac{N_{Ca}}{m_{Ca}} \quad (5-4)$$

where m_{Ca} (kg Ca/kg clay) is the concentration of calcium in the clay as dissolved Ca and in minerals that can dissolve out Ca to a concentration higher than the CCC.

The equivalent flowrate Q_{eq} is obtained from Equation 4-2 given earlier

$$Q_{eq} = 2\pi r \delta \sqrt{\frac{4D_w v}{\pi^2 r}} \quad (5-5)$$

6 Discussion

Role of minerals

It was found that soluble minerals containing divalent ions such as Ca^{2+} are very important for the long-term erosion stability of the bentonite buffer. However, only the more soluble calcium minerals such as gypsum or anhydrite can give calcium concentrations exceeding the CCC of the bentonite clay. Calcium minerals such as calcite and siderite have solubilities well below the CCC and do not significantly contribute to stabilise the bentonite clay from chemical erosion. In this report we take gypsum as the soluble calcium mineral.

Duration of fresh water intrusion

It is outside the scope of this report to assess the duration of the time fresh water can intrude to repository depths. However, in the sample calculations we have considered very long times. This is not to be interpreted that we have information that this could be the case. By general considerations it may be expected that the fresh water intrusion can be expected to be largest when a sharp ice front is located above the repository, generating very high gradients and thus flowrates. It is conceivable (to these authors) that fresh melt water will intrude also when the ice covers an extended region. Then, however, the gradient is expected to be much lower. The longer residence of the intruding fresh water will give more time for mineral weathering and the ion strength can be expected to be higher in the water that reaches repository depth.

Fracture transmissivity

We have used a broad range of transmissivity values and a high upper end of $10^{-6} \text{ m}^2 \text{ s}^{-1}$. Such values are probably much too high for a host rock where a repository may be located. The high values were used mainly for illustration purposes and should not be used as probable values. No account has been taken to the possible decrease of transmissivities due to a large ice overburden.

Possible sources of divalent ions

The main calcium containing minerals in the clays are calcium carbonate and gypsum or anhydrite. Both gypsum and anhydrite have solubilities of calcium larger than the CCC of the bentonite clay. Calcite and Siderite have solubilities lower than the CCC. The contribution to ferrous iron in the pore water from this compound would give a Fe^{2+} concentration on the order of 0.01 mmol L^{-1} . This is well below the CCC and will thus contribute only marginally to the stability of the bentonite gel.

Clay expansion into the fracture

We have not in our own models made calculations of the rate of extrusion of the clay into the fractures but have relied upon the estimates of /Pusch 1983/. In our models it is therefore assumed that clay expands into the fracture at the same rate as it is carried away by erosion and that a steady state is reached. The penetration depth will stabilise at different distances for different erosion rates. Although it would be possible to devise a model that accounts for the combined effects of clay expansion, diffusion of calcium (and other species), dissolution of gypsum and chemical erosion at the gel/water interface we have at present deemed it to give little further insights into the erosion processes, considering the complexity and the scarcity of data for such a model.

Variable aperture fractures

Fractures have very variable apertures. This causes the water to flow very unevenly in preferential flowpaths. Some flow paths can carry much more water and at higher velocities than others. Erosion can therefore be localised and not as even as our model assumes. By choosing a very wide range of transmissivities, apertures and hydraulic gradients we have tried to capture such possible variations also of local conditions in the fractures.

Some other points

Many other points have been considered in other reports and publications. We note some here because they have been raised but we deem that they are not of the highest concern or relevance for our modelling and our conclusions and are not within the scope of this report.

- *The long-term mineralogical stability of the Na-montmorillonite.* As /Arthur et al. 2005/ pointed out that, during the period of 10^6 years, possible changes of the smectite lattice chemistry resulting in alteration of montmorillonite to other dioctahedral or trioctahedral smectitic clays such beidellite, nontronite, or saponite through the slow process of amorphous substitution cannot be convincingly excluded.
- *The influence of the corrosion products of the copper canister and the iron in-fillings on the stability of the clay mineral.* /Karnland et al. 2000/ measured an increase of up to 100 ppm of Cu in the block of compacted bentonite that was placed in contact with a heated Cu tube for one year in SKB's Long Term Test of Buffer Material (LOT) experiments at the Äspö Hard Rock Laboratory (HRL). It is still unclear whether the copper cations are at the inter-laminar sites or are incorporated in the octahedrally coordinated sites.
- *The influence of the oxidation state of Fe at the octahedral sites on the rheological and chemical properties of the bentonite.* /Morcos 2003/ noted that the oxidation state of octahedral Fe in smectites can have a strong effect on the swelling pressure of bentonite. /Gates et al. 2000/ pointed out that the oxidation state of octahedral Fe can profoundly alter the cation-exchange properties, particle size, surface acidity, swelling behaviour and other properties of the smectites. /Wilson et al. 2000/ suggested that the precipitation of Fe oxyhydroxides on inter-laminar surfaces could result in a loss of cation-exchange capacity and swelling capacity of the smectites.
- *Possible increase of pH values of the pore water caused by the release of bicarbonate anions together with the release of Ca^{2+} and its influence on the stability of the bentonite buffer.* For Ca(II) poor groundwaters the pore water of the bentonite may evolve to high alkalinity of pH values of 10.5–10.8 /Bruno et al. 1999/. The charges at the edge sites are strongly dependent on pH and an increase in pH may change the charge from positive to negative and therefore decrease the strength of the EF electrostatic interactions. These interactions in turn determine the physical and chemical stabilities of the bentonite as has been discussed in Chapter 2 of this report.
- *The influence of the calcium at the CEC site on our results when the bentonite does not contain calcium minerals.* When calcium at the CEC site is to be released, other cations must be transported into the diffuse layer to compensate the charge loss. When the groundwater is fresh, probably only H^+ can exchange the calcium cations. (Exchange by other cations in the pore water will not have net effect as their loss will also decrease the ionic strength of the pore water). Then the effect of such exchanges on the charge at the edge of the clay laminae will be very complicated.

7 Conclusions

Our models are based on some basic fundamental physical and mass balance processes. It has been possible to summarise the main effects in a few very simple formulae that can be useful for performance assessment calculations.

Mechanical erosion is not expected to take place to any appreciable extent as long as the pore water in the clay has divalent cation concentrations above the CCC.

Chemical corrosion due to massive intrusion of fresh water during the aftermath of an ice age will cause chemical erosion that can be noticeable in the most transmissive fractures during the time that a very high hydraulic gradient exists.

The rate of clay erosion due to chemical effects is inversely proportional to its content of gypsum mineral and a clay with readily soluble calcium minerals such as gypsum and anhydrite could be beneficial.

References

Allard B, Larson S A, Tullborg E-L, Wikberg P, 1983. Chemistry of deep groundwaters from granitic bedrock. KBS TR-83-59, Swedish Nuclear Fuel Supply Co/Division KBS, Stockholm, Sweden.

Andersson P, Byegård J, Dershowitz B, Doe T, Hermanson J, Meier P, Tullborg E-L, Winberg A, 2002. Final report of the TRUE Block Scale project. 1. Characterisation and model development. SKB TR-02-13, Svensk Kärnbränslehantering AB.

Arthur R, Apted M, Stenhouse M, 2005. Comment on the long-term chemical and mineralogical stability of the buffer. SKI Report 2005:09, Swedish Nuclear Power Inspectorate, Stockholm, Sweden.

Boek E S, Coveney P V, Skipper N T, 1995. Monte Carlo molecular modelling studies of hydrated Li-, Na- and K-smectites: Understanding the role of potassium as a clay swelling inhibitor. *J. Am. Chem. Soc.*, 117, 12608–12617.

Bruno J, Arcos D, Duro L, 1999. Processes and features affecting the near field hydrochemistry. Groundwater-bentonite interaction. SKB TR-99-29, Svensk Kärnbränslehantering AB.

Buddemeier R, 1988. Transport of colloidal contaminants in groundwater – radionuclide migration at the Nevada Test Site. *Appl. Geochem.*, 3, 535–548.

Chilingarian G V, Vorabutr P, 1983. Chap. 11. Drilling and drilling fluids. In: *Development in Petroleum Science*. Elsevier.

Comsol, 2004. Femlab, User's guide. Version 3.1. The Comsol Co, Stockholm, Sweden.

Darley H C H, Gray G R, 1991. *Composition and Properties of Drilling and Completion Fluids*, 5th Ed. Gulf Publishing Company, London.

Evans D F, Wennerström H, 1999. *The Colloidal Domain, where physics, chemistry, biology, and technology meet*, 2nd Ed. Wiley-VCH.

Forslind E, Jacobsson A, 1973. Clay/water interactions. Final Techn. Report. Eur. Res. Off. Contract Number DAJA 37-72-C-3894.

Gates W P, Komadel P, Madejová J, Bujdák J, Stucki J W, Kirkpatrick R J, 2000. Electronic and structural properties of reduced-charge montmorillonite. *Applied Clay Science*, 16(5–6), 257–271.

Grindrod P, Peletier M, Takase H, 1999. Mechanical interaction between swelling compacted clay and fractured rock, and the leaching of clay colloids. *Engineering Geology*, 54, 159–165.

Karnland O, Sandén T, Johannesson L-E, Eriksen T E, Jansson M, Wold S, Pedersen K, Montamedi M, Rosborg B, 2000. Long term test of buffer material: Final Report on the pilot parcels. SKB TR-00-22, Svensk Kärnbränslehantering AB.

Lagaly G, Schultz O, Zimehl R, 1997. *Dispersionen und Emulsionen*. Steinkopff Verlag, Darmstadt, Germany.

Lagaly G, Ziesmer S, 2003. Colloid chemistry of clay minerals: the coagulation of montmorillonite dispersions. *Adv. Colloid Interface Sci.*, 100–102, 105–128.

Lambe T W, 1958. The structure of compacted clay. *J. Soil Mech. a. Found. Div. Proc. ASCE*, SM 2, vol. 84, Part 1.

- M'bodj O, Ariguib N K, Ayadi M T, Magnin A, 2004.** Plastic and elastic properties of the systems interstratified clay-water-electrolyte-xanthan. *J. Colloid Interface Sci*, 273, 675–684.
- Missana T, Adell A, 2000.** On the applicability of DLVO theory to the prediction of clay colloids stability. *J. Colloid Interface Sci*, 230, 150–156.
- Morcos N, 2003.** Bentonite-iron interactions in natural occurrences and in laboratory – the effect of the interactions on the properties of bentonite: a literature survey. Posiva Working Report 2003-55, Posiva Oy, Olkiluoto, Finland.
- Möri A, Alexander W R, Geckeis H, Hauser W, Schäfer T, Eikenberg J, Fierz Th, Degueldre C, Missana T, 2003.** The colloid and radionuclide retardation experiment at the Grimsel Test Site: influence of bentonite colloids on radionuclide migration in a fractured rock. *Colloid and Surfaces A: Physicochem. Eng. Aspects*, 217, 33–47.
- Neretnieks I, 1982.** Leach rates of high level wastes and spent fuel – Limiting rates as determined by backfill and bedrock conditions. *Mat. Res. Soc. Symp. Proc*, 11, 557–568. (Scientific Basis for Nuclear Waste Management V).
- Nickel S H, 1997.** A rheological approach to dispersive clays. ASTM, STP 623, J. L. Sherard and R. S. Decker (ed.), Amer. Soc. For Testing and Materials.
- Nilsson L, Moreno L, Neretnieks I, Romero L, 1991.** A resistance network model for radionuclide transport into the near field surrounding a repository for nuclear waste. SKB TR-91-30, Svensk Kärnbränslehantering AB.
- Nordman H, Vieno T, 2004.** Equivalent flowrates from canister interior into the geosphere in a KBS-3H type repository. Working Report 2004-06, Posiva Oy, Olkiluoto, Finland.
- Norrish K, 1954.** The swelling of montmorillonite. *Disc. Faraday Soc*, 18, 120.
- Norrish K, 1972.** In: *Proc. of International Clay Conference*, pp 375–383, Madrid, Spain.
- Pierre A C, 1992.** The gelation of colloidal plate-like particles. *J. Can. Ceram. Soc*, 61, 135–138.
- Pusch R, 1983.** Stability of bentonite gels in crystalline rock – physical aspects. SKBF/KBS TR-83-04, Svensk Kärnbränslehantering AB.
- Pusch R, 1999.** Clay colloid formation and release from MX-80 buffer. SKB TR-99-31, Svensk Kärnbränslehantering AB.
- Pusch R, Adey R, 1999.** Creep in buffer clay. SKB TR-99-32, Svensk Kärnbränslehantering AB.
- Ramos-Tejada M M, Arroyo F J, Perea R, Durán D G, 2001.** Scaling behaviour of the rheological properties of montmorillonite suspensions: correlation between interparticle interaction and degree of flocculation. *J. Colloid Interface Sci*, 235, 251–259.
- Rosenqvist I Th, 1955.** Investigations in the clay-electrolyte-water system. *Norg. Geot. Inst. Publ*, No. 9.
- SKB, 1999.** SR 97 – Post-closure safety, deep repository for spent fuel. Main report, Volume II. SKB TR-99-06, Svensk Kärnbränslehantering AB.
- SKB, 2004.** Interim main report of the safety assessment SR-Can. SKB TR-04-11. Svensk Kärnbränslehantering AB.
- SKB, 2004a.** Interim process report for the safety assessment SR-Can. SKB R-04-33, Svensk Kärnbränslehantering AB.

- SKB, 2004b.** Interim initial state report for the safety assessment SR-Can. SKB R-04-35, Svensk Kärnbränslehantering AB.
- SKI, 1996.** Site-94, deep repository performance assessment project. Volume I. SKI Report 96:36, Swedish Nuclear Power Inspectorate, Stockholm, Sweden.
- Stoylov S P, 1994.** Relation between stability of oxide and clay disperse systems and the electric properties of their particles. *Adv. Colloid Interface Sci*, 50, 51–78.
- van Olphen H, 1951.** Rheological phenomenon of clay soils in connection with the charge distribution on the micelles. *Discuss. Faraday Soc*, 11.
- van Olphen H, 1956.** Forces between suspended bentonite particles. *Clay and Clay Minerals*, 4, 204.
- van Olphen H, 1963.** *Introduction to Clay Colloid Chemistry*. Interscience, New York, USA.
- van Olphen H, 1977.** *An Introduction to Clay Colloid Chemistry*, 2nd Ed. John Wiley & Sons.
- Verwey E J W, Overbeek J T G, 1948.** *Theory of the Stability of Lyophobic Colloids*. Elsevier, Amsterdam, the Netherlands.
- Wanner H, Wersin P, Sierro N, 1992.** Thermodynamic modelling of bentonite-groundwater interaction and implications for near field chemistry in a repository for spent fuel. SKB TR-92-37, Svensk Kärnbränslehantering AB.
- Wieland E, Wanner H, Albinsson Y, Wersin P, Karnland O, 1994.** A surface chemical model of the bentonite-water interface and its implications for modelling the near field chemistry in a repository for spent fuel. SKB TR-94-26, Svensk Kärnbränslehantering AB.
- Wilson J, Ragnarsdottir V, Savage D, Cressey G, 2000.** The effect of iron on the stability of montmorillonite. *J. Conference Abstracts*, 5(2), 1097.